PULMONARY DISEASES

The FOXM1 inhibitor RCM-1 suppresses goblet cell metaplasia and prevents IL-13 and STAT6 signaling in allergen-exposed mice

Lifeng Sun,[1,2,3] Xiaomeng Ren,[2,3,4] I-Ching Wang,[3,5] Arun Pradhan,[2,3,4] Yufang Zhang,[2,3,4] Hannah M. Flood,[2,3] Bo Han,[1] Jeffrey A. Whitsett,[3,4] Tanya V. Kalin,[3,4] Vladimir V. Kalinichenko[2,3,4]*

Goblet cell metaplasia and excessive mucus secretion associated with asthma, cystic fibrosis, and chronic obstructive pulmonary disease contribute to morbidity and mortality worldwide. We performed a high-throughput screen to identify small molecules targeting a transcriptional network critical for the differentiation of goblet cells in response to allergens. We identified RCM-1, a nontoxic small molecule that inhibited goblet cell metaplasia and excessive mucus production in mice after exposure to allergens. RCM-1 blocked the nuclear localization and increased the proteasomal degradation of Forkhead box M1 (FOXM1), a transcription factor critical for the differentiation of goblet cells from airway progenitor cells. RCM-1 reduced airway resistance, increased lung compliance, and decreased proinflammatory cytokine production in mice exposed to the house dust mite and interleukin-13 (IL-13), which triggers goblet cell metaplasia. In cultured airway epithelial cells and in mice, RCM-1 reduced IL-13 and STAT6 (signal transducer and activator of transcription 6) signaling and prevented the expression of the STAT6 target genes *Spdef* and *Foxa3*, which are key transcriptional regulators of goblet cell differentiation. These results suggest that RCM-1 is an inhibitor of goblet cell metaplasia and IL-13 signaling, providing a new therapeutic candidate to treat patients with asthma and other chronic airway diseases.

INTRODUCTION

Asthma is a common chronic pulmonary disorder, associated with mucus hyperproduction, persistent pulmonary inflammation, airway hyperresponsiveness, and tissue remodeling (*1*). Allergen-induced activation of T helper 2 (T_H2) lymphocytes, type 2 innate lymphoid cells, and dendritic cells and eosinophilic infiltration are important components in asthma pathogenesis. In response to allergens, resident and inflammatory cells produce interleukin-4 (IL-4), IL-5, IL-13, IL-9, IL-17, IL-25, IL-33, and eotaxins that stimulate pulmonary inflammation and cause airway remodeling (*2*–*4*). Canonical T_H2 responses are initiated by cytokines and chemokines produced by respiratory epithelial cells, such as thymic stromal lymphopoietin, IL-33, and IL-25, which recruit and activate innate lymphocytes and T cells to, in turn, enhance goblet cell metaplasia and inflammation (*4*). Clinical management of asthma focuses on reducing allergen-mediated lung inflammation and alleviating the hyperresponsiveness of peripheral conducting airways (*5*), but there is a lack of therapeutic agents that directly target epithelial transcriptional networks critical for the differentiation of mucin-producing goblet cells. Pharmacological targeting of goblet cell transcription factors will provide new therapeutic opportunities for the treatment of patients with asthma and other chronic airway diseases.

Goblet cell metaplasia and mucus hypersecretion are important clinical features of asthma, cystic fibrosis, and chronic obstructive pulmonary disease. In response to allergen sensitization, goblet cells differentiate from nonciliated airway progenitor cells, including basal and Club cells (*6*–*8*). Multiple signaling and transcriptional networks influence goblet cell differentiation. These include Janus kinase (JAK) and the transcription factor signal transducer and activator of transcription 6 (STAT6), Notch, epidermal growth factor receptor (EGFR), Ras/extracellular signal–regulated kinase 1/2 (ERK1/2), and the transcription factor nuclear factor κB (NF-κB) (*7*, *9*, *10*). IL-13 acts through the IL-4 receptor to phosphorylate STAT6 and induce goblet cell metaplasia through a transcriptional network, in which SPDEF and FOXA3 are positive regulators and TTF-1 and FOXA2 are negative regulators (*11*, *12*). SPDEF is required for and sufficient to induce airway goblet cell differentiation at baseline and after aeroallergen exposure (*11*, *12*). SPDEF regulates various genes that encode factors involved in producing mucins, their glycosylation, and intracellular packaging, including *Muc5ac*, *Muc16*, *Foxa3*, and *Agr2* (*12*). FOXM1 is a transcription factor from the Forkhead box (FOX) family that is an upstream transcriptional regulator of SPDEF. FOXM1 binds to and stimulates *Spdef* promoter activity (*13*). Genetic deletion of *Foxm1* from airway Club cells inhibits SPDEF and prevents goblet cell metaplasia in response to house dust mite (HDM) allergens (*13*).

Here, we have challenged the concept that transcription factors are "undruggable" targets. Using a high-throughput screen, we identified a novel small-molecule compound [Robert Costa Memorial drug–1 (RCM-1)] that inhibits FOXM1 activity in vitro and in vivo. RCM-1 prevented goblet cell metaplasia, decreased lung inflammation, and inhibited airway hyperresponsiveness in response to HDM or recombinant IL-13. The present study suggests the feasibility of developing novel inhibitors of goblet cell metaplasia for the treatment of asthma and other chronic airway disorders associated with mucus hyperproduction.

[1]Department of Pediatrics, Shandong Provincial Hospital Affiliated to Shandong University, Jinan, Shandong 250021, China. [2]Center for Lung Regenerative Medicine, Cincinnati Children's Hospital Medical Center, Cincinnati, OH 45229, USA. [3]Division of Pulmonary Biology, Cincinnati Children's Hospital Medical Center, Cincinnati, OH 45229, USA. [4]Perinatal Institute, Cincinnati Children's Hospital Medical Center, Cincinnati, OH 45229, USA. [5]Department of Life Sciences, National Tsing Hua University, Hsinchu 30013, Taiwan.
*Corresponding author. Email: vladimir.kalinichenko@cchmc.org

RESULTS

High-throughput screen identifies the novel FOXM1 small-molecule inhibitor RCM-1

Because genetic inactivation of the *Foxm1* gene in airway Club cells effectively inhibits goblet cell metaplasia in response to HDM (*13*),

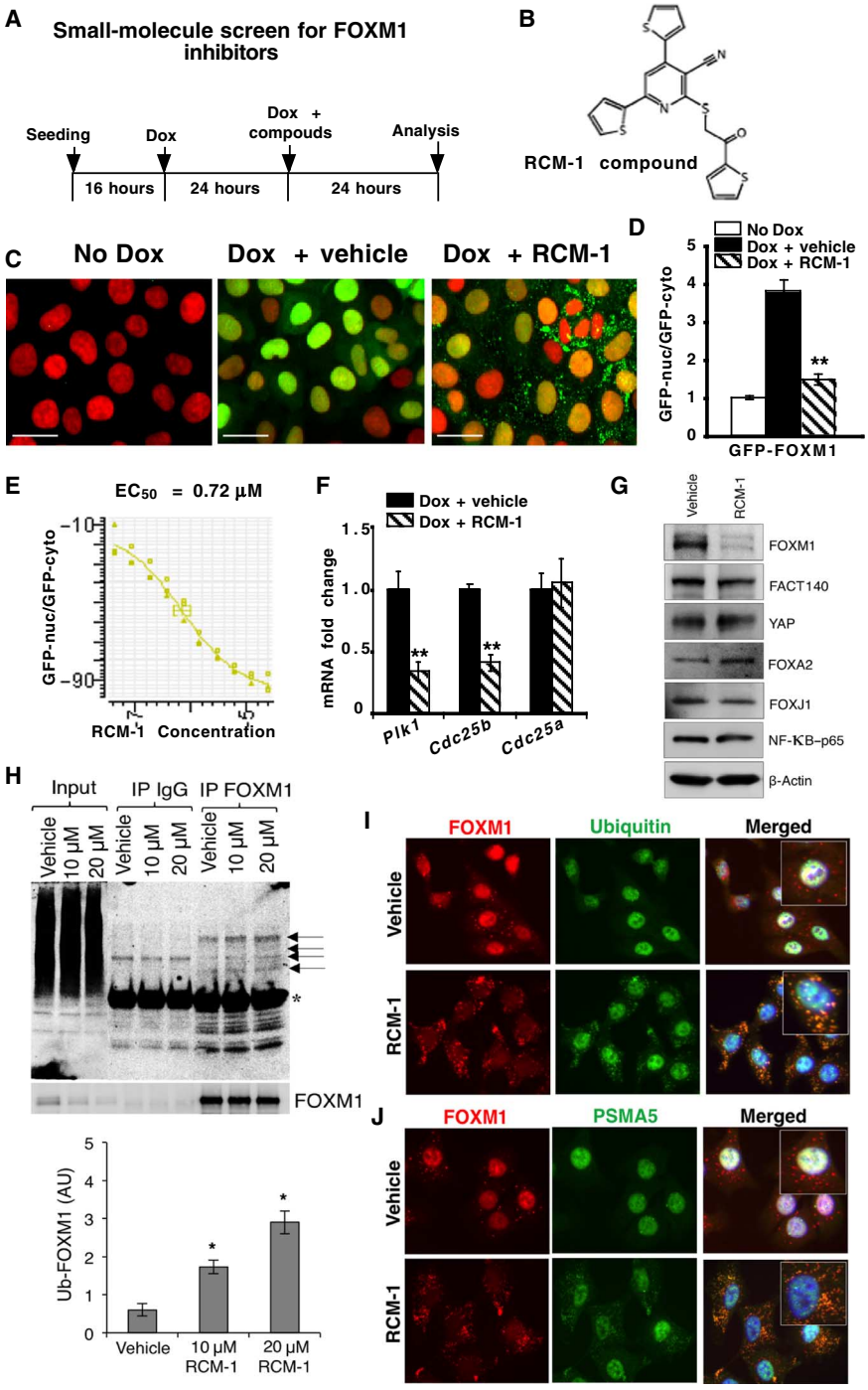

Fig. 1. Identification of the FOXM1 inhibitor RCM-1 by high-throughput screening. (**A**) Schematic of the high-throughput screen. U2OS C3 cells expressing a Dox-inducible GFP-FOXM1 construct were treated with Dox and, 24 hours later, screened with 50,000 small-molecule compounds. AU, arbitrary units. (**B**) Chemical structure of the RCM-1 compound. (**C** and **D**) RCM-1 decreased nuclear GFP-FOXM1 fluorescence. U2OS C3 cells were fixed and imaged for GFP (green) (C). Twelve random images were taken of each cell culture. DNA stain (red) and phase contrast were used to identify the nuclear-cytoplasm boundary in individual cells. Nuclear (nuc)/cytoplasmic (cyto) GFP ratio in U2OS C3 cells is shown as means ± SD (n = 200 cells per condition) (D). Scale bars, 10 μm. (**E**) Different concentrations of the RCM-1 compound were used to determine EC_{50} (n = 3 independent cell cultures). GFP-nuc, total GFP fluorescence in cell nuclei; GFP-cyto, total GFP fluorescence in cytoplasm. (**F**) Decreased mRNA abundance of FOXM1 target genes *Cdc25B* and *Plk1* was found in RCM-1–treated cells by quantitative reverse transcription polymerase chain reaction (qRT-PCR) (n = 3 independent experiments). $^{**}P < 0.01$. (**G**) Western blots show amounts of endogenous FOXM1 protein and other transcription factors in RCM-1–treated human airway epithelial cells cultured on air-liquid interface (n = 3 independent experiments). (**H**) RCM-1 increases ubiquitination of FOXM1 (arrows). FOXM1 immunoprecipitates (IP) from A549 cell lysates were Western-blotted with ubiquitin (Ub) or FOXM1 antibodies. Asterisk indicates the location of immunoglobulin G (IgG) on ubiquitin Western blot. Amounts of ubiquitin-FOXM1 were normalized to total FOXM1 (bottom) (n = 3 independent experiments). (**I** and **J**) RCM-1 induces the translocation of endogenous FOXM1 from cell nuclei to cytoplasm. FOXM1 (red) colocalizes with ubiquitin (I) and PSMA5 (J) (green) in proteasomes of RCM-1–treated A549 cells (yellow). 4′,6-Diamidino-2-phenylindole (DAPI) was used to visualize cell nuclei (n = 3 independent experiments). Scale bars, 20 μm.

we performed a high-throughput screen to identify novel small-molecule compounds that inhibit FOXM1. The screen was based on the ability of the compounds to inhibit the expression and nuclear localization of FOXM1 protein in the human osteosarcoma U2OS C3 cell line, in which doxycycline (Dox) treatment induced expression of the FOXM1 protein fused to green fluorescent protein (GFP-FOXM1) (*14*). U2OS C3 cells were treated with Dox to induce GFP-FOXM1, and 50,000 small-molecule compounds were screened for GFP fluorescence (Fig. 1A). Quantitative scanning microscopy was used to measure total GFP and nuclear/cytoplasmic GFP ratios in individual cells (fig. S1, A to C). After identification of GFP-FOXM1–inhibiting compounds, additional dose-response screens were performed to determine EC_{50} (median effective concentration). Here, we prioritized the nitrile compound RCM-1 (Fig. 1B), named in memory of the late Robert Costa, who originally identified the human *FOXM1* (also known as *HFH11*) gene. RCM-1 inhibited GFP-FOXM1 in U2OS cells with an EC_{50} of 0.72 μM (Fig. 1, C to E). Furthermore, RCM-1 inhibited the expression of FOXM1 target genes *Plk1* and *Cdc25B* (Fig. 1F), a functional readout of FOXM1 transcriptional activity (*15*). In addition to GFP-FOXM1, the RCM-1 compound decreased the abundance of endogenous FOXM1 in primary human airway epithelial cells cultured on an air-liquid interface without altering that of other transcription factors, such as YAP, FACT140, NF-κB, FOXA2, and FOXJ1 (Fig. 1G). RCM-1 inhibited FOXM1 by increasing its ubiquitination and translocation from cell nuclei to proteasomes, as demonstrated by immunoprecipitation of ubiquitinated FOXM1 isoforms (Fig. 1H) and colocalization of FOXM1 with ubiquitin (Fig. 1I) and proteasomal protein PSMA5 (Fig. 1J). Thus, RCM-1 selectively inhibits FOXM1 by increasing the protein degradation.

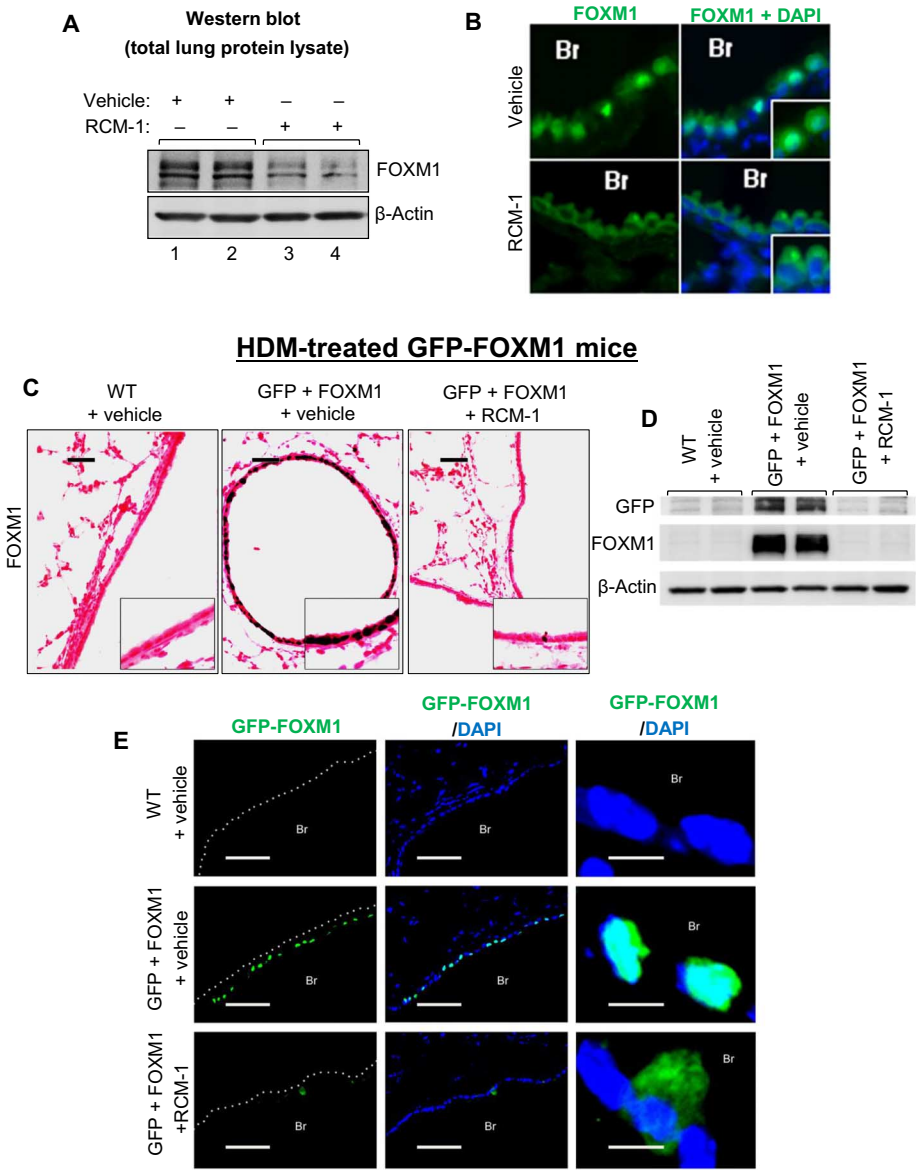

Fig. 2. RCM-1 inhibits FOXM1 in vivo. (**A**) RCM-1 inhibits FOXM1 in the mouse lung. BALB/c mice were treated with either RCM-1 or vehicle. Total lung protein was analyzed by Western blot for endogenous FOXM1 and β-actin. Each lane represents a different mouse. (**B**) GFP-FOXM1 transgenic mice were given Dox to activate the transgene and were treated with either RCM-1 or vehicle for 2 weeks. Frozen lung sections were analyzed for GFP fluorescence. RCM-1 reduces nuclear GFP-FOXM1 in bronchiolar epithelium. Scale bars, 10 μm (images are representative of five mice per treatment). (**C**) RCM-1 inhibits GFP-FOXM1 after HDM challenge. Tissue samples were prepared from lungs of Dox-treated GFP-FOXM1 transgenic mice after HDM challenge and RCM-1 treatment. Dox-treated CCSP-rtTA mice were used as controls [wild type (WT)]. Paraffin sections were stained with FOXM1 antibodies (dark brown) and counterstained with nuclear fast red (red). Scale bars, 50 μm (images are representative of four mice per treatment). (**D**) Western blot shows that RCM-1 decreases GFP and FOXM1 protein abundance in lungs of HDM-treated GFP-FOXM1 mice. Each lane represents a different mouse. (**E**) RCM-1 decreases GFP fluorescence in GFP-FOXM1 mice after HDM treatment. Frozen lung sections were stained with DAPI. Br, bronchiole. Scale bars, 50 μm (left) and 5 μm (right) (images are representative of four mice per treatment).

RCM-1 inhibits mouse and human FOXM1 in vivo

The ability of RCM-1 to inhibit FOXM1 in vivo was tested in wild-type BALB/c mice. Western blot of lung homogenates demonstrated that RCM-1 treatment decreased the abundance of endogenous FOXM1 (Fig. 2A). There was no evidence of systemic toxicity as assessed by intestinal morphology and liver, renal, and cardiac biochemical measures (fig. S2, A and B).

The ability of RCM-1 to inhibit human FOXM1 was tested using transgenic mice that express human FOXM1 fused to GFP (FOXM1-GFP) (*16*) in airway Club cells (fig. S1D). Immunostaining of lung paraffin sections from GFP-FOXM1 mice demonstrated that RCM-1 reduced both GFP and FOXM1 in airway epithelial cells (fig. S1E). Application of RCM-1 resulted in the exclusion of GFP-FOXM1 from the nuclei of bronchiolar epithelial cells (Fig. 2B), a finding consistent with RCM-1 effects in vitro (Fig. 1, C and D). RCM-1 did not affect the abundance of CCSP (a Club cell marker) or FOXA2 (fig. S1E), the latter being a transcription factor that is structurally related to FOXM1. Furthermore, RCM-1 decreased the amounts and nuclear localization of GFP-FOXM1 transgenic protein in mice exposed to the HDM allergen, as shown by immunostaining for FOXM1 (Fig. 2C), Western blot (Fig. 2D), and GFP fluorescence (Fig. 2E). Thus, RCM-1 effectively and selectively decreased the abundance of mouse and human FOXM1 proteins in vitro and in vivo.

RCM-1 inhibits goblet cell metaplasia and decreases airway resistance after HDM exposure

Because genetic inactivation of *Foxm1* protected mice from HDM-mediated pulmonary allergic responses (*13*), we tested the efficacy of RCM-1 in mice sensitized to HDM. BALB/c mice were subjected to the HDM sensitization and challenge protocol and treated with RCM-1 (Fig. 3A). Consistent with previous studies (*13*), HDM exposure altered the functional properties of lung tissue in response to methacholine, a nonselective muscarinic receptor agonist. HDM increased airway resistance to constriction (Fig. 3B). HDM also increased elastance (which measures the stiffness of the lung), tissue damping (which measures the energy dissipation in the alveoli), and tissue elastance (which measures the energy conservation in the alveoli) and decreased pulmonary compliance (which reflects the ability of the lung to expand) (Fig. 3B). RCM-1 protected lungs from HDM-induced airway hyperreactivity (as assessed by reduced airway resistance) and preserved lung function (as assessed by reduced tissue damping and elastance and increased pulmonary compliance) (Fig. 3B). Newtonian resistance (which measures resistance of central conducting airways) was not changed by RCM-1 (Fig. 3B).

Goblet cell metaplasia was inhibited by RCM-1, as shown by hematoxylin and eosin (H&E) and Alcian blue stainings (Fig. 4A).

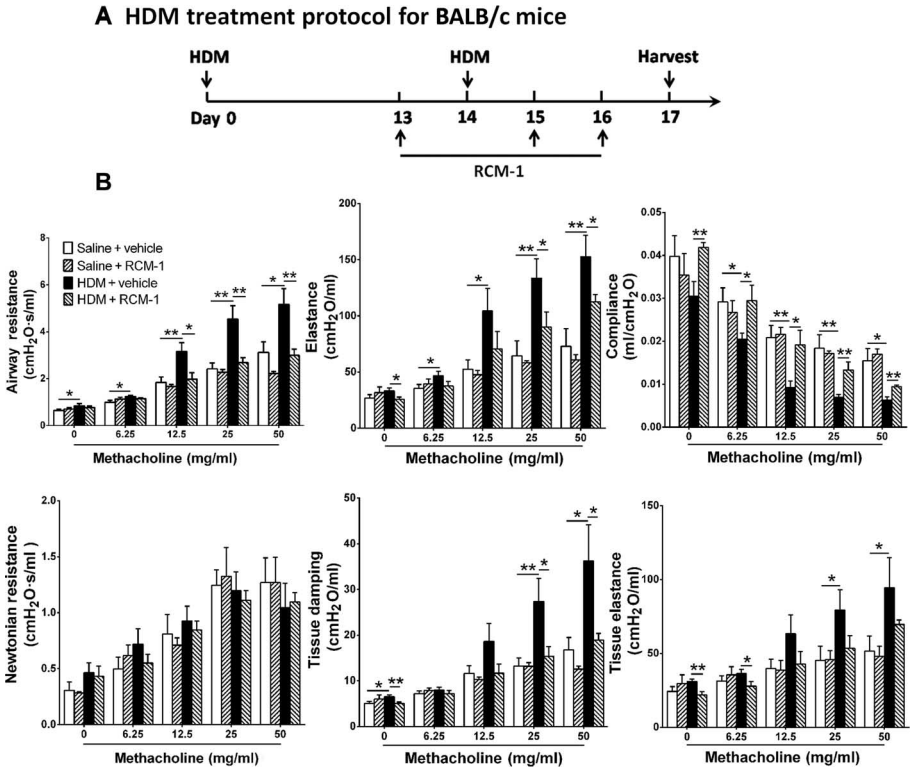

Fig. 3. RCM-1 inhibits HDM-induced airway hyperreactivity. (**A**) Experimental protocol showing the treatment of BALB/c mice with HDM and RCM-1. (**B**) RCM-1 ameliorated airway hyperreactivity induced by HDM. BALB/c mice were treated with either RCM-1 or vehicle. Airway mechanics were measured with the flexiVent system. RCM-1 treatment decreased HDM-mediated increase in airway resistance, elastance, and tissue damping. RCM-1 increased pulmonary compliance but did not change Newtonian resistance in HDM-treated lungs (n = 5 mice per treatment). *P < 0.05; **P < 0.01.

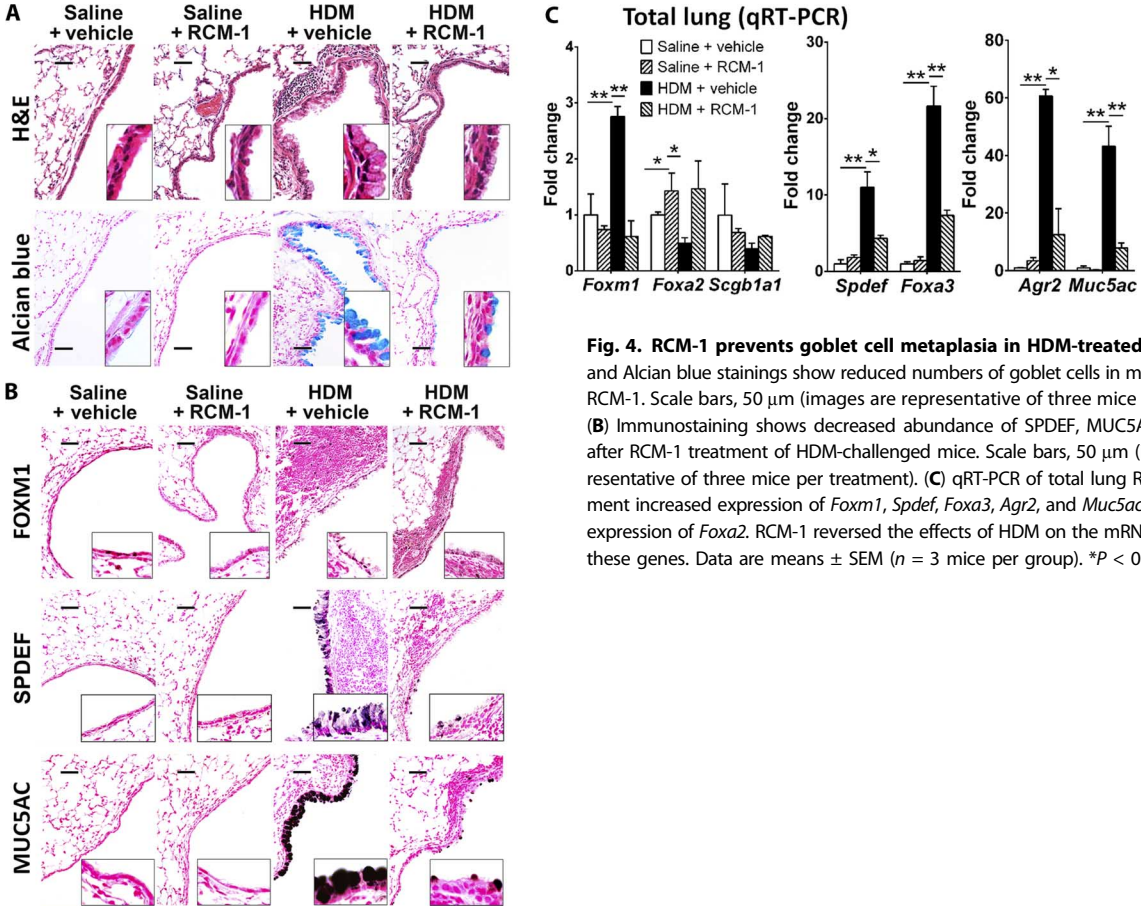

Fig. 4. RCM-1 prevents goblet cell metaplasia in HDM-treated mice. (**A**) H&E and Alcian blue stainings show reduced numbers of goblet cells in mice treated with RCM-1. Scale bars, 50 μm (images are representative of three mice per treatment). (**B**) Immunostaining shows decreased abundance of SPDEF, MUC5AC, and FOXM1 after RCM-1 treatment of HDM-challenged mice. Scale bars, 50 μm (images are representative of three mice per treatment). (**C**) qRT-PCR of total lung RNA. HDM treatment increased expression of *Foxm1*, *Spdef*, *Foxa3*, *Agr2*, and *Muc5ac* and decreased expression of *Foxa2*. RCM-1 reversed the effects of HDM on the mRNA expression of these genes. Data are means ± SEM (n = 3 mice per group). *P < 0.05; **P < 0.01.

RCM-1 decreased FOXM1 staining and mRNA abundance in response to HDM exposure (Fig. 4, B and C). RCM-1 reduced the mRNA and/or protein abundance of MUC5AC and AGR2 (goblet cell proteins that are associated with increased mucus production) (*12*), as well as that of SPDEF and FOXA3 (transcription factors that promote goblet cell metaplasia) (Fig. 4, B and C) (*12*). In contrast, RCM-1 increased the protein abundance of FOXA2 and CCSP (fig. S3A), both of which are decreased during goblet cell metaplasia (*12*). Thus, RCM-1 inhibited goblet cell metaplasia and decreased airway resistance in response to HDM exposure.

RCM-1 decreases HDM-mediated inflammation in the lung tissue

Consistent with previous studies (*13*), pulmonary HDM exposure increased the total count and changed differential counts of inflammatory cells in bronchoalveolar lavage fluid (BALF) (Fig. 5A). Pulmonary HDM exposure increased the numbers of eosinophils, neutrophils, lymphocytes, and infiltrated macrophages, as shown by the fluorescence-activated cell sorting analysis of BALF (Fig. 5B and fig. S4). Although RCM-1 did not influence the total number of inflammatory cells in BALF (Fig. 5A and fig. S3B), the numbers of neutrophils and T lymphocytes were decreased after RCM-1 treatment (Fig. 5B). RCM-1 increased the number of alveolar macrophages in BALF (Fig. 5B and fig. S4). Histological assessment of the lung tissue demonstrated that RCM-1 reduced peribronchial and perivascular infiltration by inflammatory cells and decreased alveolar thickening in HDM-treated lungs (Fig. 5C, fig. S3C, and tables S2 and S3). Furthermore, RCM-1 decreased mRNA abundance of *Ccl2* (which encodes C-C motif chemokine ligand 2), *Ccl11* (which encodes C-C motif chemokine ligand 11), *Ccl24* (which encodes C-C motif chemokine ligand 24), *Ccr2* and *Ccr3* (which encode the C-C motif chemokine receptors 2 and 3), *Acta2* (which encodes α-actin-2), and the IL-encoding mRNAs *IL-5*, *IL-13*, and *IL-33* in lung tissue, and reduced protein concentrations of IL-4, IL-5, and IL-13 in BALF (Fig. 5, D to G). RCM-1 increased interferon-γ (IFNγ) concentrations in BALF (Fig. 5G). All these genes play important roles in allergen-mediated pulmonary inflammation because they encode secreted factors that mediate dendritic cell activation (*IL-33*), T cell recruitment and airway remodeling (*IL-4*, *IL-5*, *IL-13*, *Ifng*, and *Acta2*), eosinophilic infiltration (*Ccr3*, *Ccl11*, *Ccl24*, and *IL-5*), and macrophage recruitment (*Ccr2* and *Ccl2*) (*2*–*4*). There was no effect on the expression of *IL-12p35* (which encodes IL-12a), *Cx3cl1* (which encodes C-X3-C motif ligand 1), *Ptgs2* (which encodes prostaglandin-endoperoxide synthase 2), or *Ltc4s* (which encodes leukotriene C4 synthase) (Fig. 5, D to F). Thus, RCM-1 altered HDM-mediated inflammatory responses in the lung tissue and BALF.

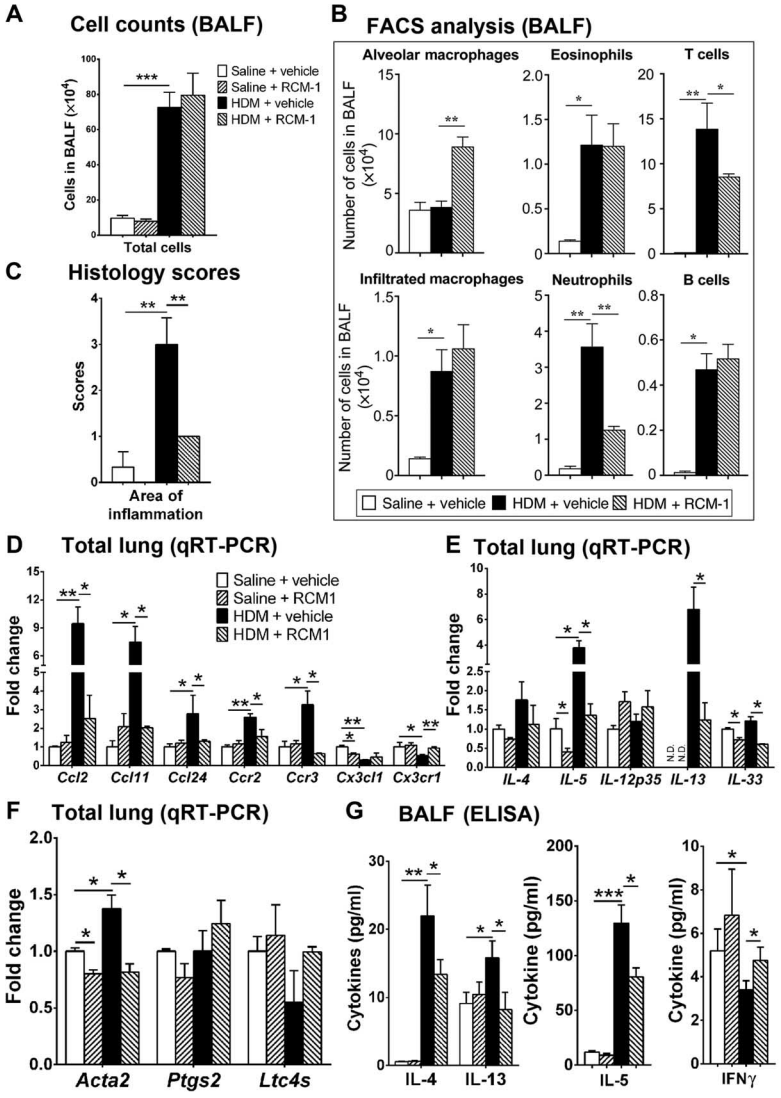

Fig. 5. Effects of RCM-1 on HDM-mediated lung inflammation. (**A**) RCM-1 did not affect the number of inflammatory cells in BALF. Cells were counted in BALF obtained from mice treated with HDM and RCM-1 (n = 6 mice per group). (**B**) BALF cells were immunostained for cell surface markers and analyzed using flow cytometry (n = 3 mice per group). (**C**) Histological assessment of lung tissue. Area of inflammation was measured using lung sections stained with H&E (n = 3 mice per group). (**D** to **F**) qRT-PCR was performed on total lung RNA to examine mRNAs encoding chemokines and cytokines, including those mediating dendritic cell activation (*IL-12p35* and *IL-33*), T_H2 cytokines (*IL-4*, *IL-5*, and *IL-13*), eosinophilic chemoattractants (*Ccr3*, *Ccl11*, and *Ccl24*), macrophage chemoattractants (*Ccr2*, *Ccl2*, *Cx3cl1*, and *Cx3cl1*), and bronchoconstrictors (*Acta2*, *Ptgs2*, and *Ltc4s*). mRNA expression was normalized to β-*actin* mRNA (n = 3 mice per group). N.D., not detected. (**G**) The Luminex Multiplex xMAP bead-based antibody assay was used to measure the concentrations of IFNγ, IL-4, IL-5, and IL-13 in BALF (n = 6 mice per group). ELISA, enzyme-linked immunosorbent assay. Data are means ± SEM. *P < 0.05; **P < 0.01; ***P < 0.001.

RCM-1 inhibits goblet cell metaplasia and airway hyperresponsiveness in response to IL-13

Because the IL-13/STAT6 signaling pathway induces goblet cell metaplasia (*11*), we tested whether RCM-1 influences IL-13/STAT6 signaling in vivo. Recombinant mouse IL-13 was administered intranasally to wild-type BALB/c mice (fig. S5A). RCM-1 decreased goblet cell metaplasia in IL-13–treated lungs, as shown by H&E and Alcian blue stainings (Fig. 6A) and immunostaining for MUC5AC, FOXM1, and SPDEF (Fig. 6B). In contrast, FOXA2 staining in airway epithelium was increased (fig. S5B). RCM-1 decreased airway resistance and improved lung function in IL-13–treated mice (Fig. 6C and fig. S6). Similar to the HDM model, RCM-1 did not influence the total cell count in BALF (Fig. 6D). RCM-1 decreased the mRNA abundance of *Foxm1*, *Spdef*, *Foxa3*, *Agr2*, and *Muc5ac* (Fig. 6E) and

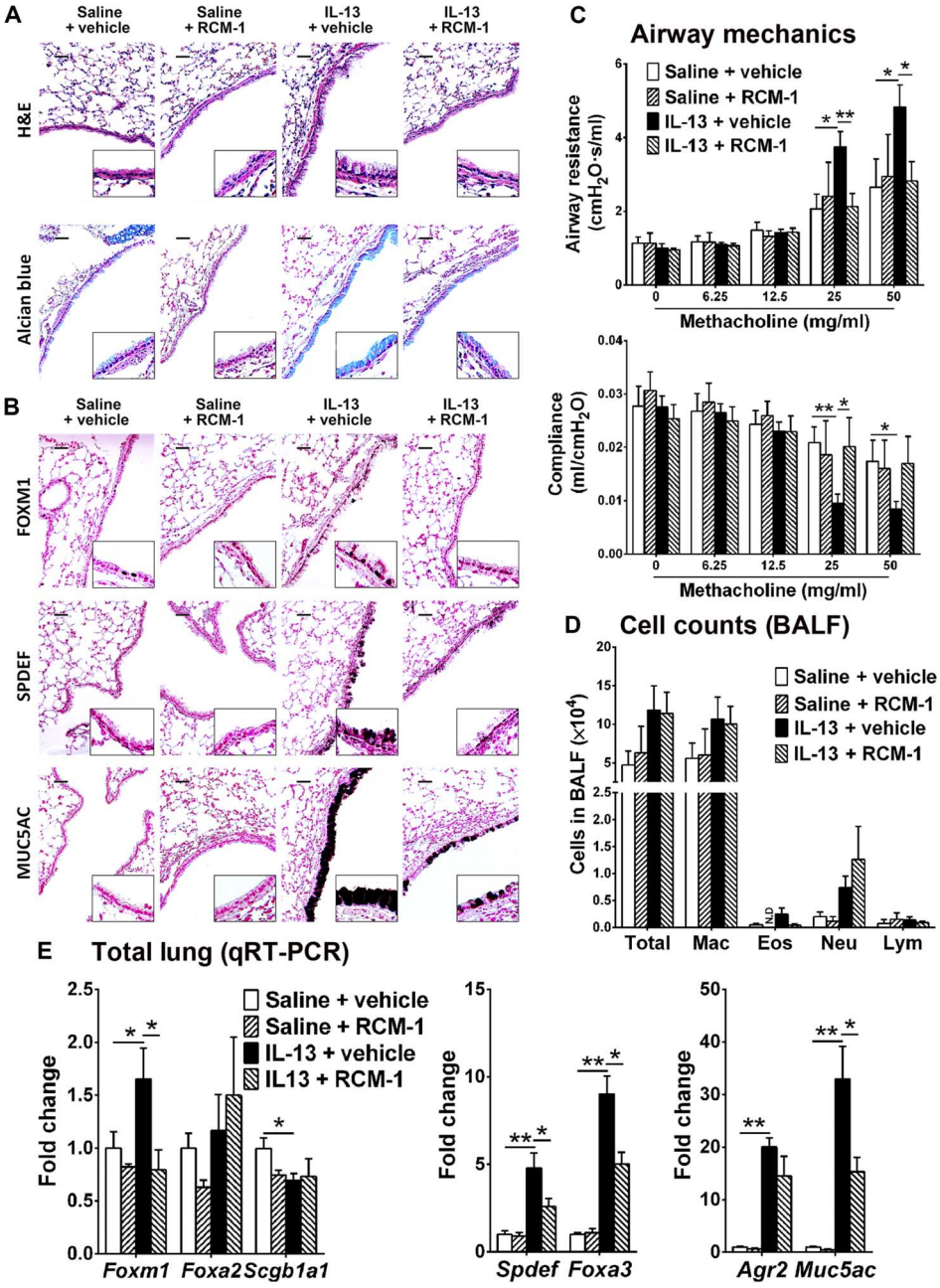

Fig. 6. RCM-1 inhibits IL-13–induced goblet cell metaplasia. (**A** and **B**) RCM-1 decreased goblet cell metaplasia after administration of IL-13. Lung paraffin sections were stained with H&E and Alcian blue (A) or used for immunostaining for FOXM1, SPDEF, and MUC5AC (B). Scale bars, 50 μm (images are representative of four mice per treatment). (**C**) The flexiVent system was used to measure airway mechanics. RCM-1 inhibited IL-13–mediated airway hyperreactivity and increased lung compliance in IL-13–treated mice (n = 5 mice per group). (**D**) RCM-1 did not change the number of inflammatory cells in BALF of IL-13–treated mice (n = 5 mice per group). Mac, macrophages; Eos, eosinophils; Neu, neutrophils; Lym, lymphocytes. (**E**) RCM-1 inhibits expression of genes associated with goblet cell metaplasia. qRT-PCR was performed on total lung RNA to measure expression of *Foxm1*, *Spdef*, *Foxa3*, *Foxa2*, *Scgb1a1*, *Agr2*, and *Muc5ac* (n = 4 mice per group). Data are means ± SEM. *P < 0.05; **P < 0.01.

reduced proinflammatory mediators in BALF and lung tissue at either the mRNA or protein levels (Fig. 7, A to C). No toxicity was observed after RCM-1 treatment, as assessed by serological analysis of blood serum (fig. S7). Thus, RCM-1 reduced goblet cell metaplasia and improved lung function after IL-13 treatment.

Because the IL-13/STAT6 and the mitogen-activated protein kinase kinase (MEK)/ERK1/2 signaling pathways induce goblet cell metaplasia in airway epithelium (*11*, *17*), we examined these pathways in RCM-1–treated lungs. RCM-1 effectively inhibited FOXM1 but did not change IL-13–induced phosphorylation of STAT6 in mouse lung tissue (Fig. 7D), human airway epithelial cells (Fig. 7E), and lung adenocarcinoma A549 cells (Fig. 7F). Furthermore, the nuclear amounts of phosphorylated STAT6 and total STAT6 were unaltered in RCM-1–treated cells (fig. S8A), indicating that RCM-1 does not affect the nuclear translocation of phosphorylated STAT6 after IL-13 exposure. In contrast, the nuclear amounts of FOXM1 were decreased in RCM-1–treated cells (fig. S8A), a finding consistent with the initial discovery of RCM-1 as a FOXM1 inhibitor (Fig. 1). Although RCM-1 did not affect the phosphorylation or nuclear translocation of STAT6, the expression of IL-13/STAT6 downstream target genes *Agr2*, *Muc5ac*, *Spdef*, and *Foxa3* was reduced (Fig. 6E), suggesting that RCM-1 acts downstream of phosphorylated STAT6 to inhibit IL-13/STAT6 signaling in airway epithelium.

The RCM-1 compound decreased the phosphorylation and total abundance of ERK1/2 in both IL-13–treated and control lungs (Fig. 7D) and in human airway epithelial cells and A549 cells independently of IL-13 (Fig. 7, E and F). RCM-1 did not alter the phosphorylation or total abundance of AKT or the total abundance of ERK5 and 14-3-3 in mouse lung tissue and in vitro (Fig. 7, D to F). Because ERK1/2 phosphorylates and activates FOXM1 in other cell types (*18*), we compared the effects of RCM-1 to the MEK inhibitor U0126. MEK is upstream of ERK1/2 in the kinase cascade (*19*), and U0126 effectively inhibited the phosphorylation of ERK1/2 but did not affect the total abundance of ERK1/2 and FOXM1 in A549 cells (fig. S8B). In contrast, RCM-1 decreased the total amounts of FOXM1 and ERK1/2 and the phosphorylation of ERK1/2 in a concentration-dependent manner (fig. S8B). Furthermore, when used at a similar concentration to RCM-1, U0126 did not influence goblet cell metaplasia (fig. S9, A and B) or total amounts of FOXM1 in HDM-exposed lungs (fig. S9D), although it decreased the total number of inflammatory cells in BALF (fig. S9C), findings distinct to the in vivo effects of RCM-1 (Figs. 4 and 5). Together, our results indicate that RCM-1 is an effective inhibitor of goblet cell metaplasia and pulmonary inflammation after HDM or IL-13 exposure.

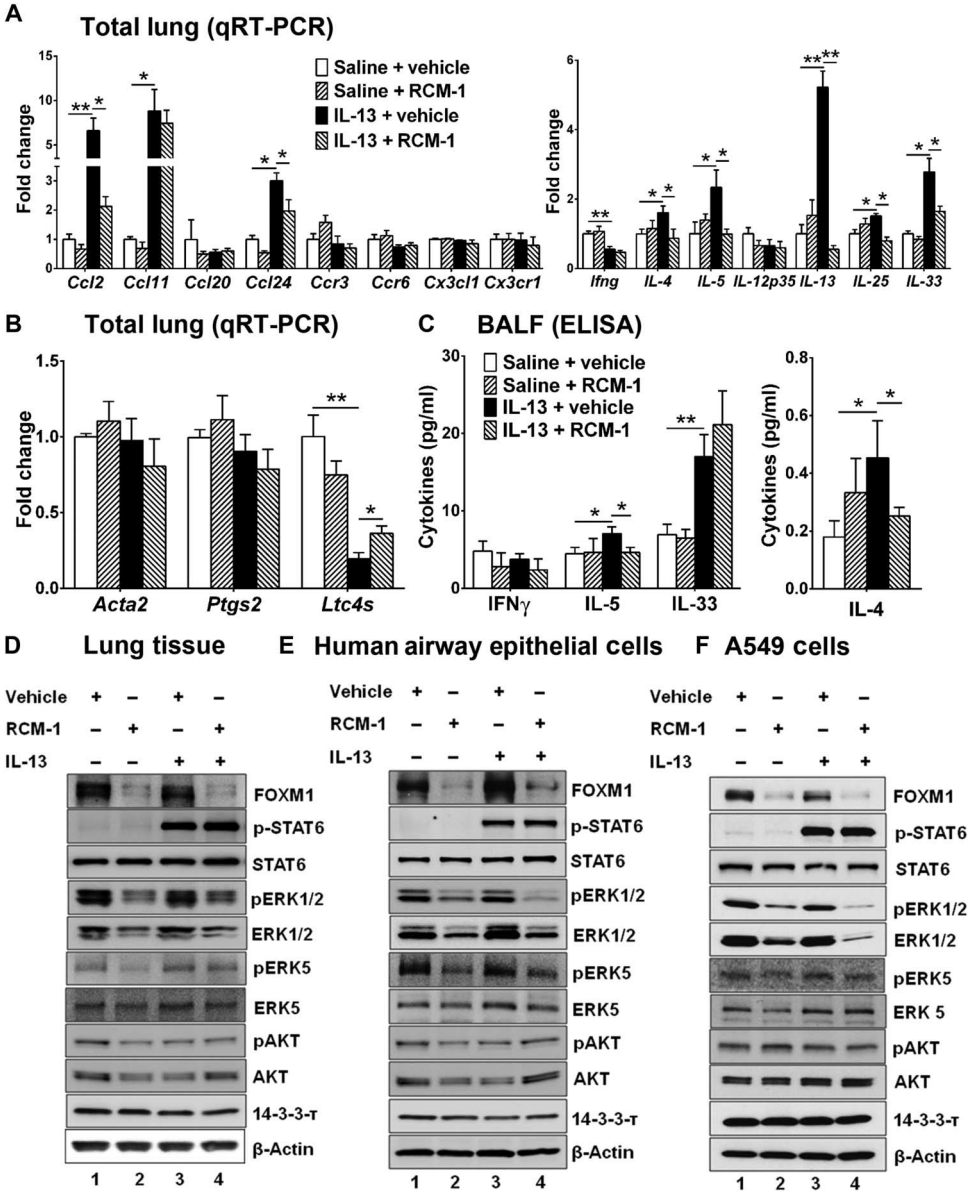

Fig. 7. RCM-1 inhibits ERK1/2 but does not change the phosphorylation of STAT6. (**A** and **B**) qRT-PCR shows altered expression of genes in RCM-1–treated lungs. qRT-PCR was performed on total lung RNA (n = 4 mice per group). (**C**) The Luminex Multiplex assay was used to measure the concentrations of IFNγ, IL-4, IL-5, and IL-33 in BALF (n = 5 mice per group). Data are means ± SEM. *P < 0.05; **P < 0.01. (**D** to **F**) RCM-1 decreases the abundance of FOXM1 and ERK1/2 and the phosphorylation (p) of ERK1/2 but does not change IL-13–induced phosphorylation of STAT6. Western blot was performed using total protein extract from mouse lung tissue (n = 3 mice per group) (D), human airway epithelial cells (n = 3 independent experiments) (E), and A549 cells (n = 5 independent experiments) (F).

DISCUSSION

FOXM1 is induced in airway epithelial cells and inflammatory cells of severe asthmatics and mice treated with ovalbumin (OVA) or HDM (*13*). FOXM1 is an important regulator of embryonic development, carcinogenesis, and organ regeneration, and its abundance is aberrantly high in chronic lung diseases (*20*–*27*). Although FOXM1 is a positive regulator of cellular proliferation (*15*, *28*, *29*), it is also present in subsets of quiescent, noncycling cells (*13*, *30*, *31*), and its role in goblet cell differentiation is independent of cell cycle regulation (*13*). Conditional deletion of the *Foxm1* gene from bronchiolar progenitor cells or inactivation of the FOXM1 protein by the membrane-penetrating ARF peptide inhibits the expression of goblet cell–specific genes and protects mice from HDM-mediated allergic responses (*13*). These studies support the concept that FOXM1 represents a potential therapeutic target to suppress mucus hyperplasia and lung inflammation.

We have previously demonstrated that the ARF peptide, a synthetic inhibitor of FOXM1, binds to and sequesters FOXM1 in the nuclei, thereby inhibiting FOXM1 transcriptional activity (*13*, *14*). Although the ARF peptide is a specific and effective inhibitor of FOXM1, its clinical applications for the treatment of chronic airway diseases are limited by the potential for immune responses against the peptide. Several pharmacological agents inhibiting FOXM1 have been previously identified, including the thiazole antibiotics siomycin A and thiostrepton (*32*–*34*) and the small-molecule compound FDI-6 (*35*). Siomycin A and thiostrepton are proteasomal inhibitors (*36*), and therefore, these compounds target multiple signaling pathways in addition to those involving FOXM1. FDI-6 inhibits binding of FOXM1 to its target DNA (*35*). Because FOXM1 and other FOX proteins share DNA binding motifs, it is likely that inhibition of *Forkhead* domain binding to DNA will influence other FOX transcription factors found in the lung, including FOXA2, FOXJ1, FOXO1, and FOXF1, leading to off-target effects. Here, we developed a strategy to target the FOXM1 protein through inhibition of its nuclear localization. Decreased nuclear localization of FOXM1 caused rapid degradation of the FOXM1 protein in cultured airway epithelial cells and in vivo, suppressing activation of FOXM1 target genes. Because FOXM1 regulates its own promoter through a positive feedback mechanism (*36*, *37*), the reduction in *Foxm1* mRNA in RCM-1–treated mice could be a consequence of the reduced abundance of the FOXM1 protein by RCM-1. Diminished nuclear localization of FOXM1 in RCM-1–treated lungs could be a result of decreased MEK/ERK1/2 signaling because ERK1/2 directly phosphorylates FOXM1, stimulating FOXM1 nuclear localization and its transcriptional activity (*18*). However, U0126, a compound inhibiting MEK/ERK1/2 signaling, did not affect abundance of FOXM1 in A549 cells and in vivo. Thus, inhibition of MEK/ERK1/2 signaling is insufficient to promote FOXM1 degradation, at least in respiratory epithelial cells. Genetic deletion of *Foxm1* from respiratory epithelial cells reduces developmental defects and prevents lung carcinogenesis in mice expressing the activated form of KRAS ($Kras^{G12D}$) (*38*–*40*), indicating that FOXM1 is required for KRAS/MEK/ERK1/2

signaling. The lack of toxicity and excellent biological responses in vivo support the concept that RCM-1 or molecules sharing its structure and function are potentially useful agents for the development of treatments for lung cancers with activating KRAS mutations, as well as pulmonary disorders associated with mucus hyperproduction and inflammation.

RCM-1 prevented goblet cell metaplasia in response to HDM and recombinant IL-13. Because FOXM1 promotes differentiation of goblet cells from airway epithelial precursors, biological effects of RCM-1 are likely related to direct inhibition of goblet cell differentiation. The lack of an effect on the phosphorylation of STAT6 by RCM-1 indicates that RCM-1 acts downstream of IL-13–mediated phosphorylation of STAT6. The reduced expression of STAT6 target genes, such as *Agr2*, *Foxa3*, and *Muc5ac*, in response to RCM-1 is consistent with inhibitory effects of RCM-1 on STAT6 transcriptional activity. Because FOXM1 transcriptionally activates SPDEF (*13*), a master regulator of goblet cell fate (*11*, *12*), it is likely that the inhibition of goblet cell differentiation by RCM-1 is mediated by its effect on the FOXM1-SPDEF regulatory cascade. In mice and humans, the gene encoding FOXM1 is expressed at early stages of goblet cell differentiation, and this expression is decreased in fully differentiated goblet cells (*13*). On the basis of the FOXM1 expression pattern in asthmatic airways, RCM-1 could be effective in inhibiting goblet cell metaplasia to prevent acute exacerbations of asthma.

RCM-1 inhibited ERK1/2 in cultured epithelial cells and in vivo. The MEK/ERK1/2 signaling pathway induces goblet cell metaplasia and allergen-mediated pulmonary inflammation (*17*, *19*). The MEK inhibitor U0126 diminishes lung inflammation in OVA-induced and HDM-mediated mouse asthma models [(*19*) and this manuscript]. Therefore, it is likely that simultaneous inhibition of FOXM1 and ERK1/2 accounts for the biological effects of RCM-1 in mouse asthma models. RCM-1 decreased airway resistance and increased compliance, findings consistent with reduced tissue stiffness and decreased inflammation. The number of T cells in BALF was reduced after RCM-1 treatment, which coincided with decreased concentrations of IL-4, IL-5, and IL-13. It is possible that RCM-1 affects the activation status of T cells. Consistent with this hypothesis, FOXM1-deficient myeloid dendritic cells exhibit reduced antigen uptake and decreased abundance of cell surface costimulatory molecules in coculture experiments with T cells (*13*). Inhibition of ERK1 can also contribute to impaired T_H2 responses in RCM-1–treated mice because genetic inactivation of ERK1 decreases T_H2 differentiation and reduced allergic inflammation (*41*). Alternatively, RCM-1 may directly inhibit the production of IL-4, IL-5, and IL-13 by activated T cells because T cell–specific deletion of *Foxm1* disrupts maturation of T cells in vivo (*42*).

In summary, we identified a novel FOXM1-inhibiting small-molecule compound, RCM-1, which effectively prevented goblet cell metaplasia, decreased airway resistance, and reduced lung inflammation in response to HDM and recombinant IL-13. Results of our studies may lead to clinical trials with FOXM1 inhibitors in patients with asthma and other chronic airway disorders.

MATERIALS AND METHODS

Mouse strains and treatment with RCM-1

Eight- to 10-week-old BALB/c mice were purchased from Charles River Laboratories. The generation of transgenic *CCSP-rtTA*$^{tg/-}$/*tetO-FOXM1*$^{tg/-}$ (GFP-FOXM1) mice has been previously described (*16*). Mice were given Dox in food chow (625 mg/kg; Harlan Teklad) to induce GFP-FOXM1 transgene. HDM extract (100 μg; Greer Laboratories) was diluted in 100 μl of saline and given by intranasal administration on days 0 and 14. The RCM-1 compound (2-{[2-oxo-2-(thiophen-2-yl) ethyl]sulfanyl}-4,6-di(thiophen-2-yl)pyridine-3- carbonitrile) was synthesized by Vitas-M Laboratory (the purity is 95%). RCM-1 was given to mice intraperitoneally [1.7 mg per kilogram of body weight in 50-μl vehicle containing 25% dimethyl sulfoxide (DMSO), 25% ethanol, and 50% corn oil] on days 13, 15, and 16. Twenty-four hours after the last HDM challenge, lungs were harvested for preparation of frozen sections and total protein. Systemic toxicity of RCM-1 was assessed by intestinal morphology and measurement of serum concentrations of total protein, albumin, liver enzymes aspartate aminotransferase and alanine aminotransferase, alkaline phosphatase, blood urea nitrogen, and creatine phosphokinase. The U0126 compound (Calbiochem) was given intraperitoneally (1.7 mg per kilogram of body weight in 50-μl vehicle containing 3% DMSO, 6% Tween 80, and 91% corn oil) on days 13, 15, and 16.

For IL-13 treatment, recombinant murine IL-13 (0.5 μg; BioLegend) was diluted in saline and given by intranasal administration on days 1, 3, and 4. RCM-1 or vehicle was given by intraperitoneal injection on days 0, 2, and 4. On day 5, lungs were harvested for paraffin embedding and preparation of RNA and protein. The flexiVent system was used to measure airway mechanics, as described (*43*, *44*). Methacholine was delivered using an Aeroneb nebulizer (SCIREQ). Serological testing of blood serum was performed in the animal facility of Cincinnati Children's Research Foundation. Animal studies were approved by the Animal Care and Use Committee of Cincinnati Children's Research Foundation.

Cell culture of human bronchial epithelial cells

Primary normal human bronchial epithelial (NHBE) cells were purchased from Lonza and used at passages 2 to 3. For air-liquid interface cultures, NHBE cells were seeded on semipermeable Transwell membranes (pore size, 0.4 μm; diameter, 12 mm) coated with collagen (BD Biosciences). Cells were grown submerged in growth basal medium (Lonza). After 2 days, cells were exposed to air, and B-ALI differentiation medium (B-ALI SingleQuots kit, Lonza) was added to the basal chamber. All cultures were maintained at 37°C in a humidified atmosphere of 5% CO_2. One hour after RCM-1 treatment (1 μM), cells were treated with recombinant human IL-13 (10 ng/ml; eBioscience Inc.) and harvested 2 to 24 hours later.

Small-molecule screen for FOXM1 inhibitors

Generation of U2OS C3 cells containing Dox-inducible GFP-FOXM1 fusion protein was previously described (*14*). For the small-molecule screen, 2000 cells were plated per each well. Sixteen hours later, Dox (1 μg/ml) was added to the cell culture. After 24 hours, 50,000 small-molecule compounds (4 μg/ml, diluted in 0.1% DMSO) from the chemical library of the Genome Research Institute (University of Cincinnati) were added in Dox-containing medium. Cells were fixed 24 hours later and scanned for GFP using scanning PerkinElmer Opera imaging system.

qRT-PCR, Western blot, and measurements of cytokines in BALF

RNA was prepared from whole lung tissue. A StepOnePlus real-time PCR system (Applied Biosystems) was used as described previously (*45*–*47*). Samples were amplified with TaqMan gene expression mastermix (Applied Biosystems) combined with inventoried TaqMan gene expression assays for the gene of interest (table S1). Reactions were analyzed in triplicate. Expression was normalized to β-*actin* mRNA. BALF concentrations of IL-4, IL-5, IL-13, IFNγ, and IL-33

were measured by the Luminex Multiplex xMAP bead-based antibody assay according to the manufacturer's recommendations. Western blot analysis was performed as described previously (*48–51*) using either total lung protein or protein extract from human airway epithelial cells (Lonza) or A549 cells (American Type Culture Collection). The following antibodies were used for Western blotting: FOXM1 (C-20), FACT140 (28734), NF-κB–p65 (372), STAT6 (C-9), and β-actin (C-11) (all from Santa Cruz Biotechnology); YAP (4912S), phospho-STAT6 (9631), ERK1/2 (4695), phospho-ERK1/2 (pERK1/2) (4370), AKT (4687), phospho-AKT (3787), ERK5 (3552), and pERK5 (3371) (all from Cell Signaling Technology); FOXA2 (WRAB-1200) and FOXJ1 (WMAB-319) (both from Seven Hills Bioreagents); 14-3-3 (Bethyl Laboratories); and GFP (A11122, Life Technologies). The signals from the primary antibodies were amplified by horseradish peroxidase (HRP)–conjugated secondary antibodies (Bio-Rad) and detected using the Enhanced Chemiluminescence Plus substrate (Amersham Pharmacia Biotech).

Histological examination and immunohistochemical staining

Five-micrometer paraffin sections were stained with H&E and Alcian blue or used for immunohistochemistry, as described previously (*52–54*). The following antibodies were used for immunostaining: FOXM1 (1:500; C-20 and H-300, Santa Cruz Biotechnology), Clara cell–secreted protein (1:2000; WRAB-CCSP, Seven Hill Bioreagents), FOXA2 (1:2000; WRAB-FOXA2, Seven Hills Bioreagents), SPDEF (1:2000; generated in the laboratory of J. A. Whitsett) (*12*), and MUC5AC (1:500; 45M1, Abcam). Antibody-antigen complexes were detected using biotinylated secondary antibody followed by avidin-biotin-HRP complex and 3,3′-diaminobenzidine substrate (all from Vector Laboratories) (*55*, *56*). Sections were counterstained with nuclear fast red. Immunofluorescence staining was performed as described (*57*, *58*). GFP fluorescence from the *GFP-FOXM1* transgene was detected in frozen lung sections. Fluorescence images were obtained using a Zeiss AxioPlan2 microscope equipped with an Axiocam MRm digital camera and Axiovision 4.3 software (Carl Zeiss). Histological assessment and scoring were done in the pathology laboratory of Cincinnati Children's Hospital using criteria described in table S2.

Flow cytometry

Inflammatory cells were stained as previously described (*13*, *52*) using the following antibodies: anti-CD45 (clone 30-F11, eBioscience), anti–T cell receptor β (TCRβ) (H57-597, eBioscience), anti-CD68 (FA-11, BioLegend), anti–Siglec F (E50-2440, BD Biosciences), anti-Ly6G (1A8, BioLegend), anti-Ly6C (HK1.4, BioLegend), and anti-CD19 (1D3, BD Biosciences). Dead cells were excluded using 7-aminoactinomycin-D stain (eBioscience). The following cell surface markers were used to identify specific cell types: neutrophils ($CD45^+TCR\beta^-CD68^-Ly6G^{hi}Ly6C^+SSC^{med}$), alveolar macrophages ($CD45^+CD68^+$Siglec $F^+FSC^{hi}SSC^{hi}$), T cells ($CD45^+Ly6G^-TCR\beta^+SSC^{lo}$), infiltrated macrophages ($CD45^+$Siglec F^-CD68^+), eosinophils ($CD45^+CD68^-$Siglec F^+SSC^{hi}), and B cells ($CD45^+$Siglec $F^-CD68^-CD19^+SSC^{lo}$). Staining was performed after incubation with Fc block (anti-mouse CD16/CD32; clone 93, eBioscience). Stained cells were analyzed using LSR II flow cytometer.

Statistical analysis

Student's *t* test and one-way analysis of variance (ANOVA) were used to determine statistical significance. Right skewed measurements were log-transformed to meet normality assumption before analyses. P values <0.05 were considered significant. Values were expressed as means ± SEM. For the high-throughput screen, z factor was used to determine statistical significance (z values >0.5 were considered significant).

SUPPLEMENTARY MATERIALS

www.sciencesignaling.org/cgi/content/full/10/475/eaai8583/DC1

Fig. S1. RCM-1 decreases FOXM1 abundance in U2OS cells and pulmonary airways.
Fig. S2. Lack of toxicity after RCM-1 treatment.
Fig. S3. RCM-1 protects bronchiolar epithelial cells from HDM-mediated effects.
Fig. S4. Identification of inflammatory cells in BALF of HDM-treated mice.
Fig. S5. RCM-1 protects bronchiolar epithelial cells from IL-13–mediated decreases in the abundance of FOXA2.
Fig. S6. Lung mechanics in mice treated with IL-13 and RCM-1.
Fig. S7. Lack of toxicity of RCM-1 in IL-13–treated mice.
Fig. S8. RCM-1 inhibits nuclear accumulation of FOXM1 protein in A549 cells.
Fig. S9. U0126 decreases lung inflammation but does not affect goblet cell metaplasia or the abundance of FOXM1.
Table S1. TaqMan assays for qRT-PCR.
Table S2. Histological evaluation of inflammatory responses in lung tissue.
Table S3. Histology scores of lung tissue from HDM-treated mice.

REFERENCES AND NOTES

1. C. Ober, T.-C. Yao, The genetics of asthma and allergic disease: A 21st century perspective. *Immunol. Rev.* **242**, 10–30 (2011).
2. C. A. Herrick, K. Bottomly, To respond or not to respond: T cells in allergic asthma. *Nat. Rev. Immunol.* **3**, 405–412 (2003).
3. S. A. Saenz, M. Noti, D. Artis, Innate immune cell populations function as initiators and effectors in Th2 cytokine responses. *Trends Immunol.* **31**, 407–413 (2010).
4. H. Hammad, B. N. Lambrecht, Barrier epithelial cells and the control of type 2 immunity. *Immunity* **43**, 29–40 (2015).
5. J. A. Krishnan, S. Q. Davis, E. T. Naureckas, P. Gibson, B. H. Rowe, An umbrella review: Corticosteroid therapy for adults with acute asthma. *Am. J. Med.* **122**, 977–991 (2009).
6. J. R. Rock, M. W. Onaitis, E. L. Rawlins, Y. Lu, C. P. Clark, Y. Xue, S. H. Randell, B. L. M. Hogan, Basal cells as stem cells of the mouse trachea and human airway epithelium. *Proc. Natl. Acad. Sci. U.S.A.* **106**, 12771–12775 (2009).
7. J. R. Rock, X. Gao, Y. Xue, S. H. Randell, Y.-Y. Kong, B. L. M. Hogan, Notch-dependent differentiation of adult airway basal stem cells. *Cell Stem Cell* **8**, 639–648 (2011).
8. E. L. Rawlins, T. Okubo, Y. Xue, D. M. Brass, R. L. Auten, H. Hasegawa, F. Wang, B. L. M. Hogan, The role of Scgb1a1$^+$ Clara cells in the long-term maintenance and repair of lung airway, but not alveolar, epithelium. *Cell Stem Cell* **4**, 525–534 (2009).
9. T. Doherty, D. Broide, Cytokines and growth factors in airway remodeling in asthma. *Curr. Opin. Immunol.* **19**, 676–680 (2007).
10. J. W. Tyner, E. Y. Kim, K. Ide, M. R. Pelletier, W. T. Roswit, J. D. Morton, J. T. Battaile, A. C. Patel, G. A. Patterson, M. Castro, M. S. Spoor, Y. You, S. L. Brody, M. J. Holtzman, Blocking airway mucous cell metaplasia by inhibiting EGFR antiapoptosis and IL-13 transdifferentiation signals. *J. Clin. Invest.* **116**, 309–321 (2006).
11. K.-S. Park, T. R. Korfhagen, M. D. Bruno, J. A. Kitzmiller, H. Wan, S. E. Wert, G. K. Khurana Hershey, G. Chen, J. A. Whitsett, SPDEF regulates goblet cell hyperplasia in the airway epithelium. *J. Clin. Invest.* **117**, 978–988 (2007).
12. G. Chen, T. R. Korfhagen, Y. Xu, J. Kitzmiller, S. E. Wert, Y. Maeda, A. Gregorieff, H. Clevers, J. A. Whitsett, SPDEF is required for mouse pulmonary goblet cell differentiation and regulates a network of genes associated with mucus production. *J. Clin. Invest.* **119**, 2914–2924 (2009).
13. X. Ren, T. A. Shah, V. Ustiyan, Y. Zhang, J. Shinn, G. Chen, J. A. Whitsett, T. V. Kalin, V. V. Kalinichenko, FOXM1 promotes allergen-induced goblet cell metaplasia and pulmonary inflammation. *Mol. Cell. Biol.* **33**, 371–386 (2013).
14. V. V. Kalinichenko, M. Major, X. Wang, V. Petrovic, J. Kuechle, H. M. Yoder, B. Shin, A. Datta, P. Raychaudhuri, R. H. Costa, Foxm1b transcription factor is essential for development of hepatocellular carcinomas and is negatively regulated by the p19ARF tumor suppressor. *Genes Dev.* **18**, 830–850 (2004).
15. R. H. Costa, V. V. Kalinichenko, M. L. Major, P. Raychaudhuri, New and unexpected: Forkhead meets ARF. *Curr. Opin. Genet. Dev.* **15**, 42–48 (2005).
16. I.-C. Wang, Y. Zhang, J. Snyder, M. J. Sutherland, M. S. Burhans, J. M. Shannon, H. J. Park, J. A. Whitsett, V. V. Kalinichenko, Increased expression of FoxM1 transcription factor in respiratory epithelium inhibits lung sacculation and causes Clara cell hyperplasia. *Dev. Biol.* **347**, 301–314 (2010).
17. V. V. Polosukhin, J. M. Cates, W. E. Lawson, A. P. Milstone, A. G. Matafonov, P. P. Massion, J. W. Lee, S. H. Randell, T. S. Blackwell, Hypoxia-inducible factor-1 signalling promotes goblet cell hyperplasia in airway epithelium. *J. Pathol.* **224**, 203–211 (2011).

18. R. Y. M. Ma, T. H. K. Tong, A. M. S. Cheung, A. C. C. Tsang, W. Y. Leung, K.-M. Yao, Raf/MEK/MAPK signaling stimulates the nuclear translocation and transactivating activity of FOXM1c. *J. Cell Sci.* **118**, 795–806 (2005).
19. W. Duan, J. H. Chan, C. H. Wong, B. P. Leung, W. S. F. Wong, Anti-inflammatory effects of mitogen-activated protein kinase kinase inhibitor U0126 in an asthma mouse model. *J. Immunol.* **172**, 7053–7059 (2004).
20. W. Korver, M. W. Schilham, P. Moerer, M. J. van den Hoff, K. Dam, W. H. Lamers, R. H. Medema, H. Clevers, Uncoupling of S phase and mitosis in cardiomyocytes and hepatocytes lacking the winged-helix transcription factor trident. *Curr. Biol.* **8**, 1327–1330 (1998).
21. K. Krupczak-Hollis, X. Wang, V. V. Kalinichenko, G. A. Gusarova, I.-C. Wang, M. B. Dennewitz, H. M. Yoder, H. Kiyokawa, K. H. Kaestner, R. H. Costa, The mouse Forkhead Box m1 transcription factor is essential for hepatoblast mitosis and development of intrahepatic bile ducts and vessels during liver morphogenesis. *Dev. Biol.* **276**, 74–88 (2004).
22. I.-M. Kim, S. Ramakrishna, G. A. Gusarova, H. M. Yoder, R. H. Costa, V. V. Kalinichenko, The forkhead box M1 transcription factor is essential for embryonic development of pulmonary vasculature. *J. Biol. Chem.* **280**, 22278–22286 (2005).
23. Y. Liu, R. T. Sadikot, G. R. Adami, V. V. Kalinichenko, S. Pendyala, V. Natarajan, Y.-y. Zhao, A. B. Malik, FoxM1 mediates the progenitor function of type II epithelial cells in repairing alveolar injury induced by *Pseudomonas aeruginosa*. *J. Exp. Med.* **208**, 1473–1484 (2011).
24. D. Balli, Y. Zhang, J. Snyder, V. V. Kalinichenko, T. V. Kalin, Endothelial cell–specific deletion of transcription factor FoxM1 increases urethane-induced lung carcinogenesis. *Cancer Res.* **71**, 40–50 (2011).
25. C. Bolte, Y. Zhang, A. York, T. V. Kalin, J. E. J. Schultz, J. D. Molkentin, V. V. Kalinichenko, Postnatal ablation of Foxm1 from cardiomyocytes causes late onset cardiac hypertrophy and fibrosis without exacerbating pressure overload-induced cardiac remodeling. *PLOS ONE* **7**, e48713 (2012).
26. D. Balli, X. Ren, F.-S. Chou, E. Cross, Y. Zhang, V. V. Kalinichenko, T. V. Kalin, Foxm1 transcription factor is required for macrophage migration during lung inflammation and tumor formation. *Oncogene* **31**, 3875–3888 (2012).
27. V. Ustiyan, Y. Zhang, A.-K. T. Perl, J. A. Whitsett, T. V. Kalin, V. V. Kalinichenko, β-Catenin and Kras/Foxm1 signaling pathway are critical to restrict Sox9 in basal cells during pulmonary branching morphogenesis. *Dev. Dyn.* **245**, 590–604 (2016).
28. C. Bolte, Y. Zhang, I.-C. Wang, T. V. Kalin, J. D. Molkentin, V. V. Kalinichenko, Expression of Foxm1 transcription factor in cardiomyocytes is required for myocardial development. *PLOS ONE* **6**, e22217 (2011).
29. A. Sengupta, V. V. Kalinichenko, K. E. Yutzey, FoxO1 and FoxM1 transcription factors have antagonistic functions in neonatal cardiomyocyte cell-cycle withdrawal and *IGF1* gene regulation. *Circ. Res.* **112**, 267–277 (2013).
30. T. V. Kalin, V. Ustiyan, V. V. Kalinichenko, Multiple faces of FoxM1 transcription factor: Lessons from transgenic mouse models. *Cell Cycle* **10**, 396–405 (2011).
31. X. Wang, D. Bhattacharyya, M. B. Dennewitz, Y. Zhou, V. V. Kalinichenko, R. Lepe, R. H. Costa, Rapid hepatocyte nuclear translocation of the Forkhead Box M1B (FoxM1B) transcription factor causes a transient increase in size of regenerating transgenic hepatocytes. *Gene Expr.* **11**, 149–162 (2003).
32. S. K. Radhakrishnan, U. G. Bhat, D. E. Hughes, I.-C. Wang, R. H. Costa, A. L. Gartel, Identification of a chemical inhibitor of the oncogenic transcription factor forkhead box M1. *Cancer Res.* **66**, 9731–9735 (2006).
33. J. M.-M. Kwok, S. S. Myatt, C. M. Marson, R. C. Coombes, D. Constantinidou, E. W.-F. Lam, Thiostrepton selectively targets breast cancer cells through inhibition of forkhead box M1 expression. *Mol. Cancer Ther.* **7**, 2022–2032 (2008).
34. N. S. Hegde, D. A. Sanders, R. Rodriguez, S. Balasubramanian, The transcription factor FOXM1 is a cellular target of the natural product thiostrepton. *Nat. Chem.* **3**, 725–731 (2011).
35. M. V. Gormally, T. S. Dexheimer, G. Marsico, D. A. Sanders, C. Lowe, D. Matak-Vinković, S. Michael, A. Jadhav, G. Rai, D. J. Maloney, A. Simeonov, S. Balasubramanian, Suppression of the FOXM1 transcriptional programme via novel small molecule inhibition. *Nat. Commun.* **5**, 5165 (2014).
36. M. Halasi, A. L. Gartel, Targeting FOXM1 in cancer. *Biochem. Pharmacol.* **85**, 644–652 (2013).
37. X.-H. Cheng, M. Black, V. Ustiyan, T. Le, L. Fulford, A. Sridharan, M. Medvedovic, V. V. Kalinichenko, J. A. Whitsett, T. V. Kalin, SPDEF inhibits prostate carcinogenesis by disrupting a positive feedback loop in regulation of the Foxm1 oncogene. *PLOS Genet.* **10**, e1004656 (2014).
38. I.-C. Wang, J. Snyder, Y. Zhang, J. Lander, Y. Nakafuku, J. Lin, G. Chen, T. V. Kalin, J. A. Whitsett, V. V. Kalinichenko, Foxm1 mediates cross talk between Kras/mitogen-activated protein kinase and canonical Wnt pathways during development of respiratory epithelium. *Mol. Cell. Biol.* **32**, 3838–3850 (2012).
39. I.-C. Wang, V. Ustiyan, Y. Zhang, Y. Cai, T. V. Kalin, V. V. Kalinichenko, Foxm1 transcription factor is required for the initiation of lung tumorigenesis by oncogenic $Kras^{G12D}$. *Oncogene* **33**, 5391–5396 (2014).
40. V. V. Kalinichenko, T. V. Kalin, Is there potential to target FOXM1 for 'undruggable' lung cancers? *Expert Opin. Ther. Targets* **19**, 865–867 (2015).
41. N. Goplen, Z. Karim, L. Guo, Y. Zhuang, H. Huang, M. M. Gorska, E. Gelfand, G. Pages, J. Pouyssegur, R. Alam, ERK1 is important for Th2 differentiation and development of experimental asthma. *FASEB J.* **26**, 1934–1945 (2012).
42. L. Xue, L. Chiang, B. He, Y.-Y. Zhao, A. Winoto, FoxM1, a forkhead transcription factor is a master cell cycle regulator for mouse mature T cells but not double positive thymocytes. *PLOS ONE* **5**, e9229 (2010).
43. V. Ustiyan, S. E. Wert, M. Ikegami, I.-C. Wang, T. V. Kalin, J. A. Whitsett, V. V. Kalinichenko, Foxm1 transcription factor is critical for proliferation and differentiation of Clara cells during development of conducting airways. *Dev. Biol.* **370**, 198–212 (2012).
44. T. V. Kalin, L. Meliton, A. Y. Meliton, X. Zhu, J. A. Whitsett, V. V. Kalinichenko, Pulmonary mastocytosis and enhanced lung inflammation in mice heterozygous null for the Foxf1 gene. *Am. J. Respir. Cell Mol. Biol.* **39**, 390–399 (2008).
45. V. Ustiyan, I.-C. Wang, X. Ren, Y. Zhang, J. Snyder, Y. Xu, S. E. Wert, J. L. Lessard, T. V. Kalin, V. V. Kalinichenko, Forkhead box M1 transcriptional factor is required for smooth muscle cells during embryonic development of blood vessels and esophagus. *Dev. Biol.* **336**, 266–279 (2009).
46. Y. Cai, C. Bolte, T. Le, C. Goda, Y. Xu, T. V. Kalin, V. V. Kalinichenko, FOXF1 maintains endothelial barrier function and prevents edema after lung injury. *Sci. Signal.* **9**, ra40 (2016).
47. A. V. Dharmadhikari, J. J. Sun, K. Gogolewski, B. L. Carofino, V. Ustiyan, M. Hill, T. Majewski, P. Szafranski, M. J. Justice, R. S. Ray, M. E. Dickinson, V. V. Kalinichenko, A. Gambin, P. Stankiewicz, Lethal lung hypoplasia and vascular defects in mice with conditional *Foxf1* overexpression. *Biol. Open* **5**, 1595–1606 (2016).
48. A. Pradhan, V. Ustiyan, Y. Zhang, T. V. Kalin, V. V. Kalinichenko, Forkhead transcription factor FoxF1 interacts with Fanconi anemia protein complexes to promote DNA damage response. *Oncotarget* **7**, 1912–1926 (2016).
49. D. Malin, I.-M. Kim, E. Boetticher, T. V. Kalin, S. Ramakrishna, L. Meliton, V. Ustiyan, X. Zhu, V. V. Kalinichenko, Forkhead box F1 is essential for migration of mesenchymal cells and directly induces integrin-beta3 expression. *Mol. Cell. Biol.* **27**, 2486–2498 (2007).
50. H. Xia, X. Ren, C. S. Bolte, V. Ustiyan, Y. Zhang, T. A. Shah, T. V. Kalin, J. A. Whitsett, V. V. Kalinichenko, Foxm1 regulates resolution of hyperoxic lung injury in newborns. *Am. J. Respir. Cell Mol. Biol.* **52**, 611–621 (2015).
51. A. M. Hoggatt, J. R. Kim, V. Ustiyan, X. Ren, T. V. Kalin, V. V. Kalinichenko, B. P. Herring, The transcription factor Foxf1 binds to serum response factor and myocardin to regulate gene transcription in visceral smooth muscle cells. *J. Biol. Chem.* **288**, 28477–28487 (2013).
52. X. Ren, Y. Zhang, J. Snyder, E. R. Cross, T. A. Shah, T. V. Kalin, V. V. Kalinichenko, Forkhead box M1 transcription factor is required for macrophage recruitment during liver repair. *Mol. Cell. Biol.* **30**, 5381–5393 (2010).
53. X. Ren, V. Ustiyan, A. Pradhan, Y. Cai, J. A. Havrilak, C. S. Bolte, J. M. Shannon, T. V. Kalin, V. V. Kalinichenko, FOXF1 transcription factor is required for formation of embryonic vasculature by regulating VEGF signaling in endothelial cells. *Circ. Res.* **115**, 709–720 (2014).
54. A. D. Hoffmann, X. H. Yang, O. Burnicka-Turek, J. D. Bosman, X. Ren, J. D. Steimle, S. A. Vokes, A. P. McMahon, V. V. Kalinichenko, I. P. Moskowitz, *Foxf* genes integrate *tbx5* and hedgehog pathways in the second heart field for cardiac septation. *PLOS Genet.* **10**, e1004604 (2014).
55. V. V. Kalinichenko, Y. Zhou, B. Shin, D. Beer-Stoltz, S. C. Watkins, J. A. Whitsett, R. H. Costa, Wild type levels of the mouse *Forkhead Box f1* gene are essential for lung repair. *Am. J. Physiol. Lung Cell Mol. Physiol.* **282**, L1253–L1265 (2002).
56. I.-M. Kim, Y. Zhou, S. Ramakrishna, D. E. Hughes, J. Solway, R. H. Costa, V. V. Kalinichenko, Functional characterization of evolutionary conserved DNA regions in forkhead box f1 gene locus. *J. Biol. Chem.* **280**, 37908–37916 (2005).
57. V. V. Kalinichenko, G. A. Gusarova, B. Shin, R. Costa, The forkhead box F1 transcription factor is expressed in brain and head mesenchyme during mouse embryonic development. *Gene Expr. Patterns* **3**, 153–158 (2003).
58. J. Xu, H. Liu, Y. Lan, B. J. Aronow, V. V. Kalinichenko, R. Jiang, A Shh-Foxf-Fgf18-Shh molecular circuit regulating palate development. *PLOS Genet.* **12**, e1005769 (2016).

Acknowledgments: We thank A. Maher for excellent editorial assistance, C. Bolte for helpful comments, and L. Fei for help with statistical analyses. **Funding:** This work was supported by NIH grants HL84151 (to V.V.K.), HL123490 (to V.V.K.), HL132849 (to T.V.K.), and CA142724 (to T.V.K.); American Cancer Society research scholar grant RSG-13-325 (to T.V.K.); National Health Research Institutes of Taiwan grant NHRI-EX105-10309BC (to I-C.W.); and Ministry of Science and Technology of Taiwan grant MOST102-2628-B-007-003-MY3 (to I-C.W.). **Author contributions:** Conception and design: L.S., I-C.W., J.A.W., T.V.K., and V.V.K.; analysis and interpretation: L.S., X.R., I-C.W., A.P., Y.Z., H.M.F., B.H., and V.V.K.; drafting the manuscript for important intellectual content: L.S., J.A.W., T.V.K., and V.V.K. **Competing interests:** The authors declare that they have no competing interests. **Data and materials availability:** The patent application 62/396,992 on RCM-1 was filed by Cincinnati Children's Hospital and is pending.

Submitted 22 August 2016
Accepted 31 March 2017
Published 18 April 2017
10.1126/scisignal.aai8583

Citation: L. Sun, X. Ren, I.-C. Wang, A. Pradhan, Y. Zhang, H. M. Flood, B. Han, J. A. Whitsett, T. V. Kalin, V. V. Kalinichenko, The FOXM1 inhibitor RCM-1 suppresses goblet cell metaplasia and prevents IL-13 and STAT6 signaling in allergen-exposed mice. *Sci. Signal.* **10**, eaai8583 (2017).

Science Signaling
AAAS

The FOXM1 inhibitor RCM-1 suppresses goblet cell metaplasia and prevents IL-13 and STAT6 signaling in allergen-exposed mice

Lifeng Sun, Xiaomeng Ren, I-Ching Wang, Arun Pradhan, Yufang Zhang, Hannah M. Flood, Bo Han, Jeffrey A. Whitsett, Tanya V. Kalin and Vladimir V. Kalinichenko (April 18, 2017)
Science Signaling **10** (475), . [doi: 10.1126/scisignal.aai8583]

Science Signaling (ISSN 1937-9145) is published weekly, except the last December, by the American Association for the Advancement of Science, 1200 New York Avenue, NW, Washington, DC 20005.

Science Signaling
AAAS

www.sciencesignaling.org/cgi/content/full/10/475/eaai8583/DC1

Supplementary Materials for

The FOXM1 inhibitor RCM-1 suppresses goblet cell metaplasia and prevents IL-13 and STAT6 signaling in allergen-exposed mice

Lifeng Sun, Xiaomeng Ren, I-Ching Wang, Arun Pradhan, Yufang Zhang, Hannah M. Flood, Bo Han, Jeffrey A. Whitsett, Tanya V. Kalin, Vladimir V. Kalinichenko*

*Corresponding author. Email: vladimir.kalinichenko@cchmc.org

Published 18 April 2017, *Sci. Signal.* **10**, eaai8583 (2017)
DOI: 10.1126/scisignal.aai8583

This PDF file includes:

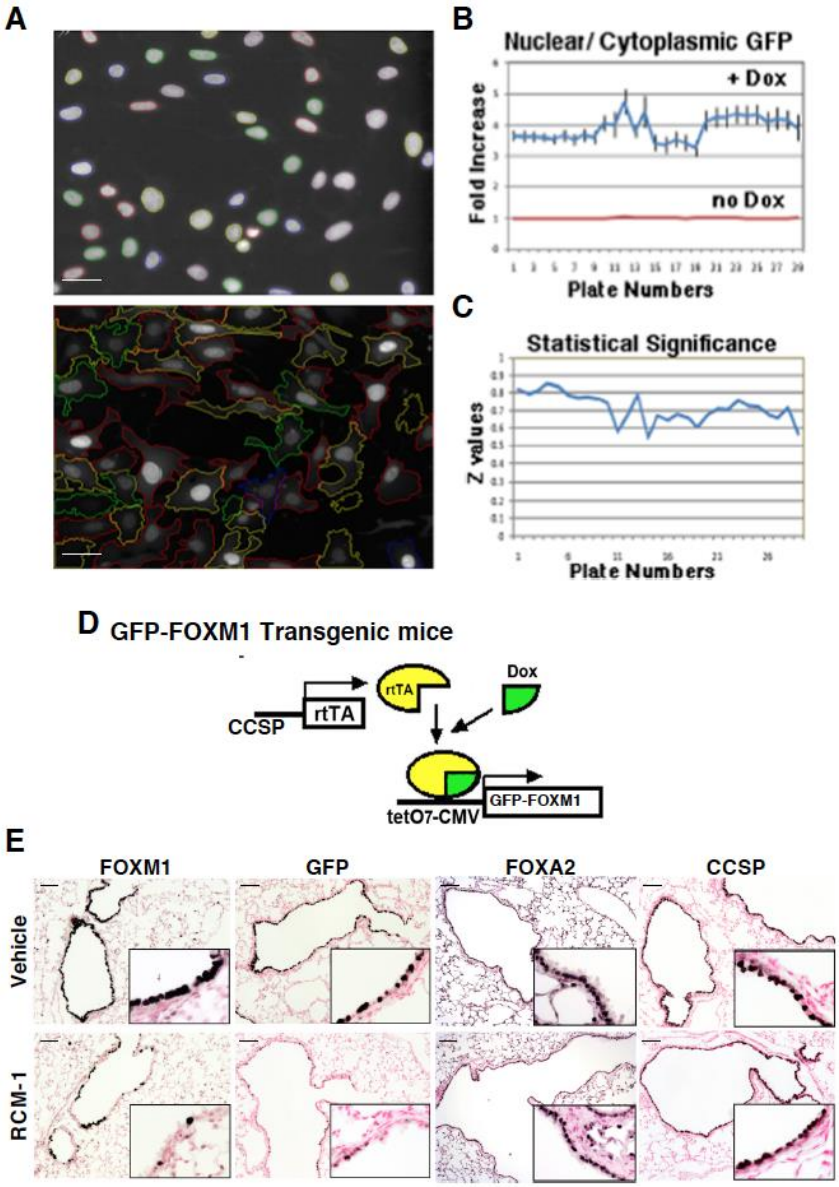

Fig. S1. RCM-1 decreases FOXM1 abundance in U2OS cells and pulmonary airways. (A–C) Images (A) show nuclei and cell boundaries in U2OS C3 reporter cells treated with Dox. A scanning imaging system was used to measure GFP in nuclei and cytoplasm of 200 randomly selected cells. Nuclear/cytoplasmic GFP ratios were determined for each individual cell. Statistical significance is shown as mean ± standard deviation (B) and *Z values* (C) calculated from 30 different cell culture plates. Scale bars are 20μm. (D) Schematic diagram of a Dox-inducible system in *CCSP-rtTA/tetO-FOXM1* double transgenic mice (GFP-FOXM1). (E) RCM-1 decreases the expression of the GFP-FOXM1 transgene in bronchiolar epithelium. GFP-FOXM1 mice were given Dox to activate transgene. 24-hr later, mice were treated with either RCM-1 or vehicle for 2 weeks (i.p. with 48-hr intervals). RCM-1 decreased immunostaining for FOXM1 and GFP. CCSP and FOXA2 were not changed. Scale bars are 100μm (images are representative of 3 mice per treatment).

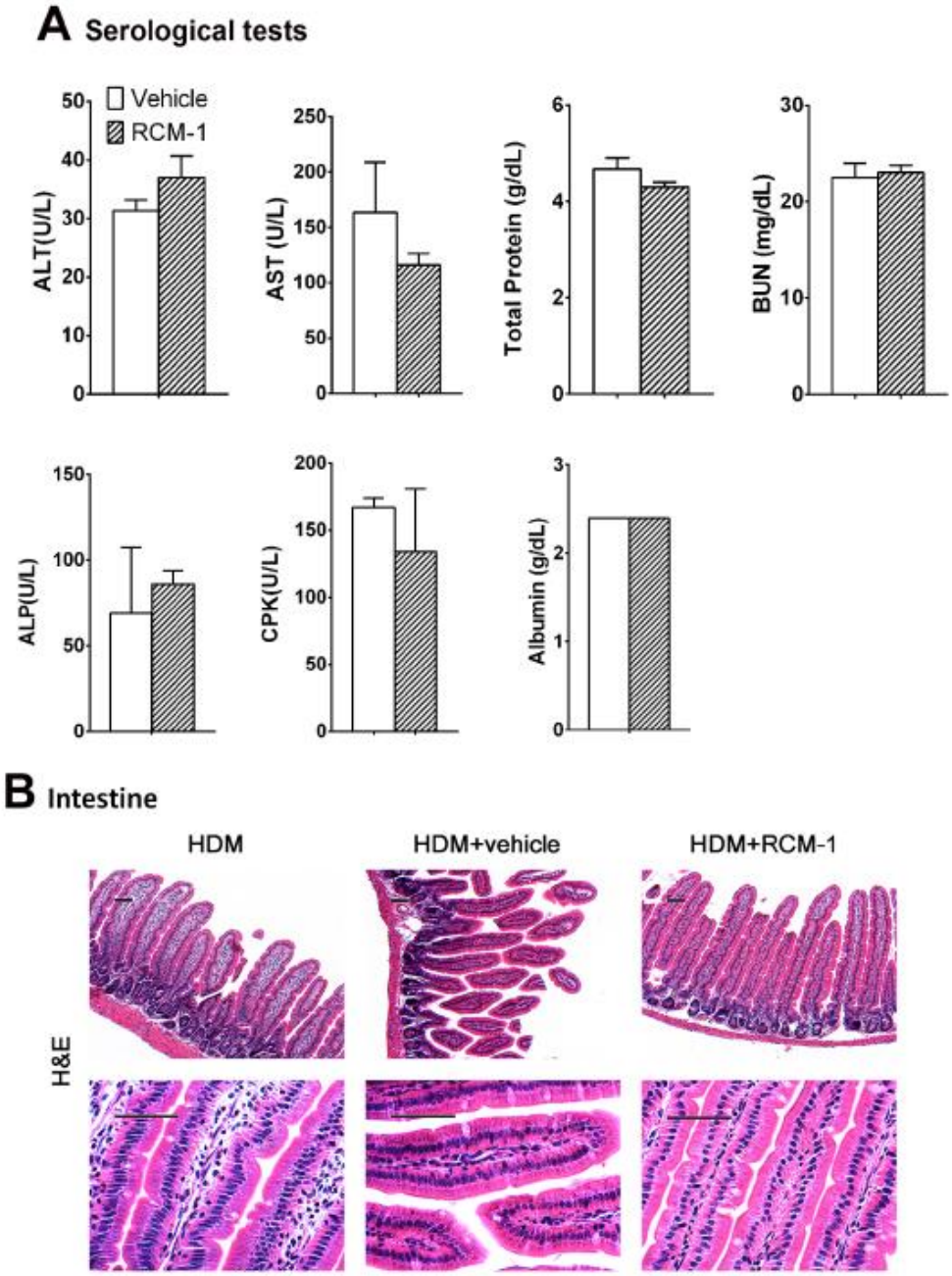

Fig. S2. Lack of toxicity after RCM-1 treatment. (A) BALB/c mice were treated with either RCM-1 or vehicle three times with 48hr intervals. Blood serum was obtained 24hr after the last RCM-1 administration. Serological tests of blood serum show that RCM-1 did not affect the liver enzymes ALT and AST, blood urea nitrogen (BUN), creatine phosphokinase (CPK), alkaline phosphatase (ALP), albumin and total protein (n=4 mice per group; *, $P < 0.05$; **, $P < 0.01$). Data are shown as means ± standard errors of the means (SEM). (B) H&E staining shows that RCM-1 did not change histology of the intestine. Scale bars are 100μm (top panels) and 50μm (bottom panels) (images are representative of 3 mice per treatment).

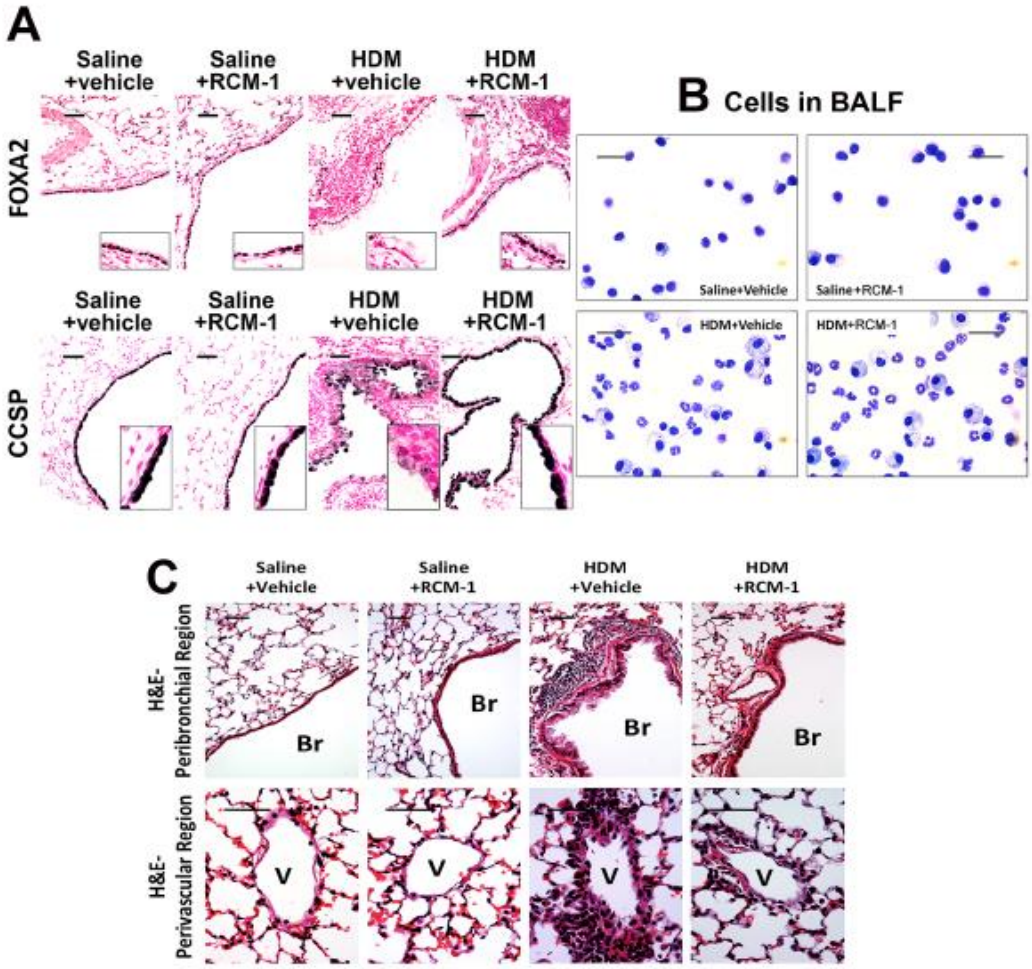

Fig. S3. RCM-1 protects bronchiolar epithelial cells from HDM-mediated effects. (A) Lung paraffin sections were immunostained for FOXA2 and CCSP (dark brown). Slides were counterstained with nuclear fast red (red). HDM was given to BALB/c mice by intranasal administration on days 0 and 14. RCM-1 was given by intraperitoneal injection on days 13, 15 and 16. Lungs were harvested 72h after the last HDM challenge. Scale bars are 50μm (images are representative of 3 mice per treatment). (B) Images show the presence of inflammatory cells in BALF obtained from mice treated with HDM or saline. Scale bars are 10μm (images are representative of 3 mice per treatment.) (C) H&E staining shows increased pulmonary inflammation after HDM treatment. RCM-1 decreases inflammatory response in HDM-treated lungs (images are representative of 4 mice per treatment). Scale bars are 50μm. Abbreviations: Br, bronchiole; V, blood vessel.

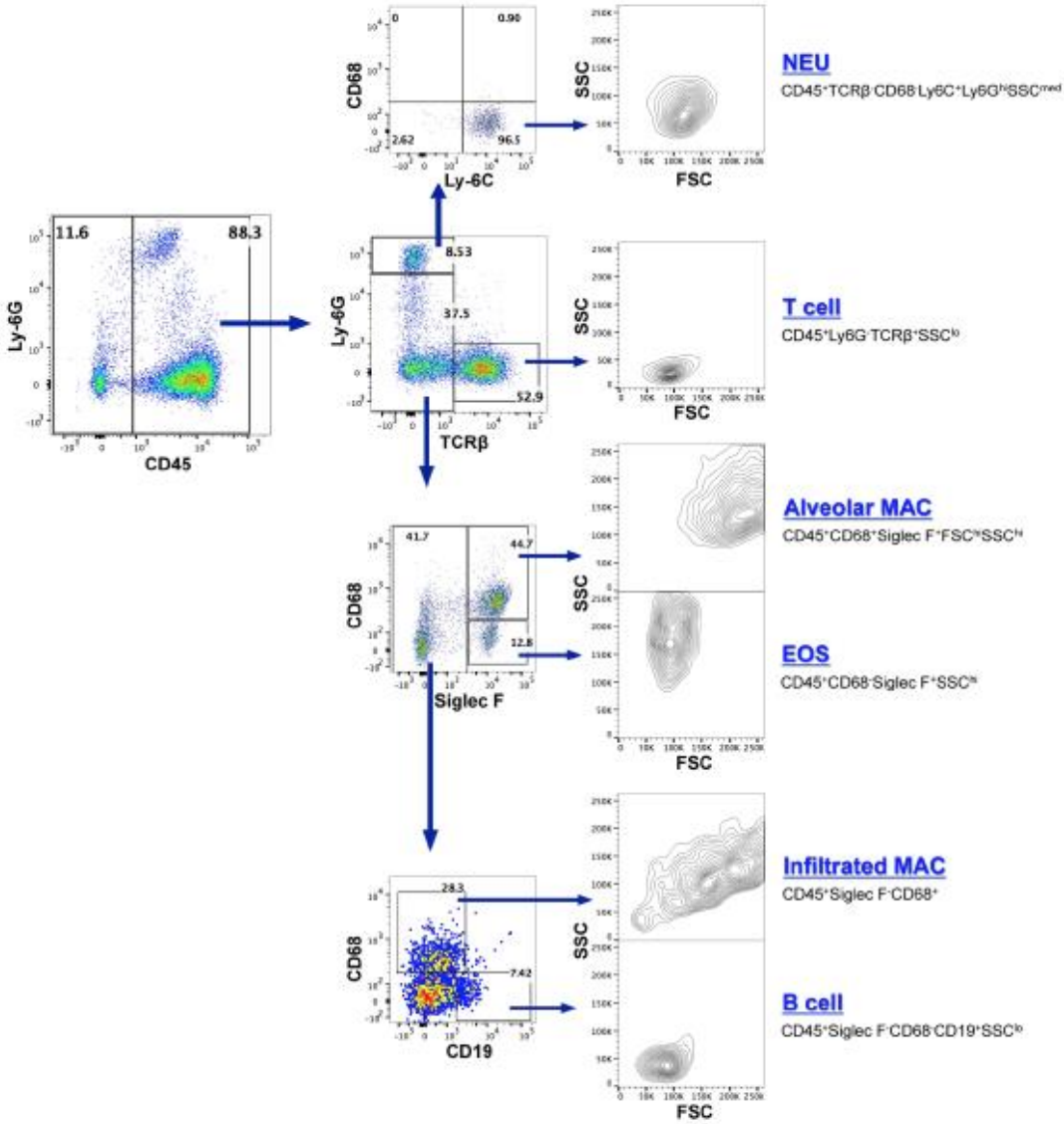

Fig. S4. Identification of inflammatory cells in BALF of HDM-treated mice. HDM was given to BALB/c mice by intranasal administration on days 0 and 14. RCM-1 was given by intraperitoneal injection on days 13, 15 and 16. BALF was obtained 72h after the last HDM challenge and inflammatory cells were identified by Flow cytometry. Following cell surface markers were used to identify specific cell types: neutrophils ($CD45^{+}TCR\beta^{-}CD68^{-}Ly6G^{hi}Ly6C^{+}SSC^{med}$), alveolar macrophages ($CD45^{+}CD68^{+}$Siglec F^{+} FSC^{hi} SSC^{hi}), T cells ($CD45^{+}Ly6G^{-}TCR\beta^{+}SSC^{lo}$), infiltrated macrophages ($CD45^{+}$ Siglec F^{-} $CD68^{+}$), eosinophils ($CD45^{+}CD68^{-}$Siglec $F^{+}SSC^{hi}$), B cells ($CD45^{+}$ Siglec$F^{-}CD68^{-}CD19^{+}SSC^{lo}$). Images are representative of 3 mice per treatment.

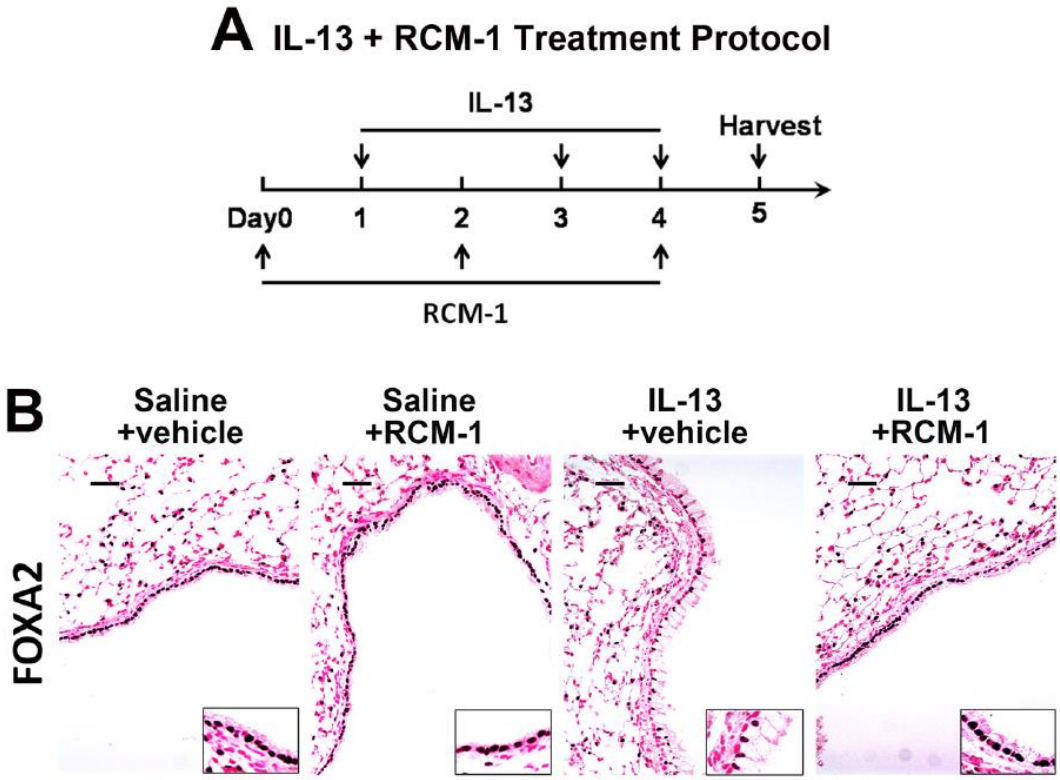

Fig. S5. RCM-1 protects bronchiolar epithelial cells from IL-13–mediated decreases in the abundance of FOXA2. (A) Experimental protocol shows the treatment of BALB/c mice with RCM-1 and recombinant mouse IL-13. IL-13 was given by intranasal administration on days 1, 3 and 4. RCM-1 was given by i.p. injection on days 0, 2 and 4. Mice were sacrificed on day 5. (B) Lung paraffin sections were used for immunostaining with FOXA2 antibodies (brown). Slides were counterstained with nuclear fast red (red). Scale bars are 50μm (images are representative of 4 mice per treatment).

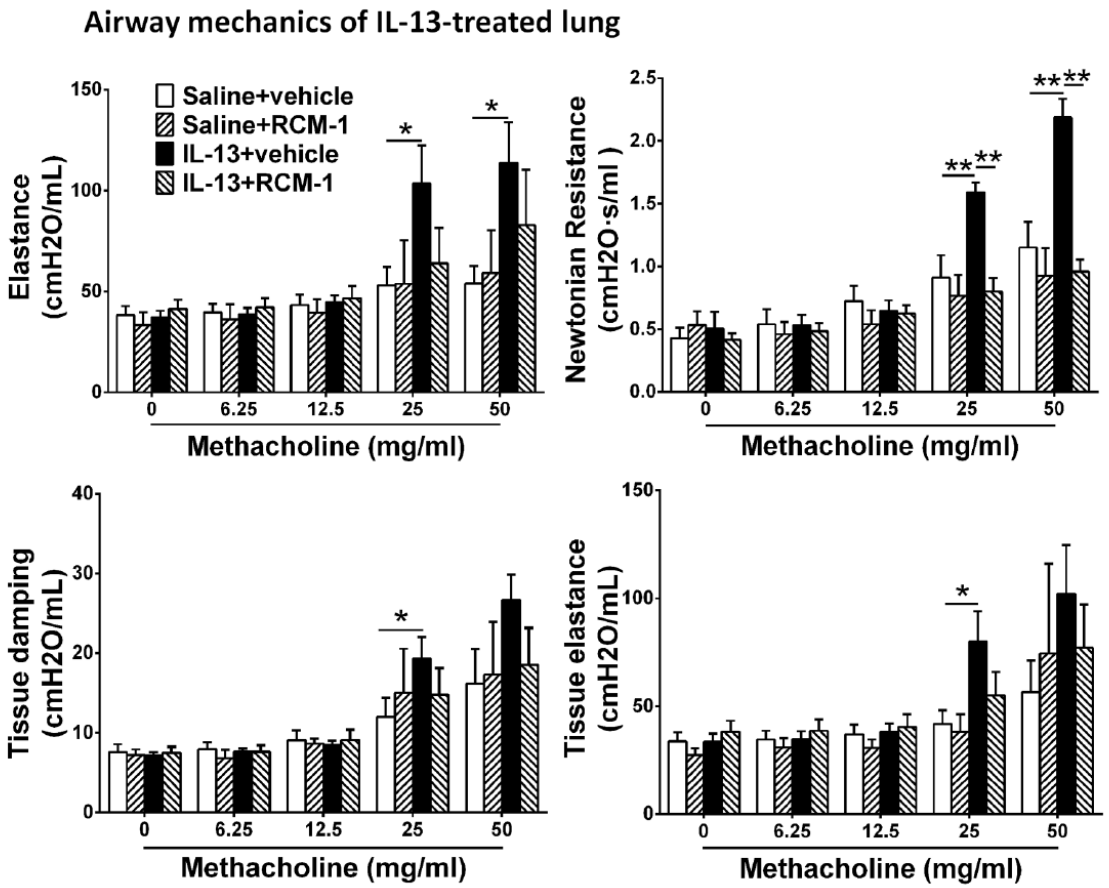

Fig. S6. Lung mechanics in mice treated with IL-13 and RCM-1. IL-13 was given to BALB/c mice by intranasal administration on days 1, 3 and 4. RCM-1 was given by i.p. injection on days 0, 2 and 4. FlexiVent was used to measure lung mechanics on day 5. IL-13 increased the elastance, Newtonian resistance, tissue damping and tissue elastance. RCM-1 significantly reduced IL-13-mediated increase in Newtonian resistance (n=5 mice per group; *, $P<0.05$; **, $P<0.01$). Data are shown as means ± standard errors of the means (SEM).

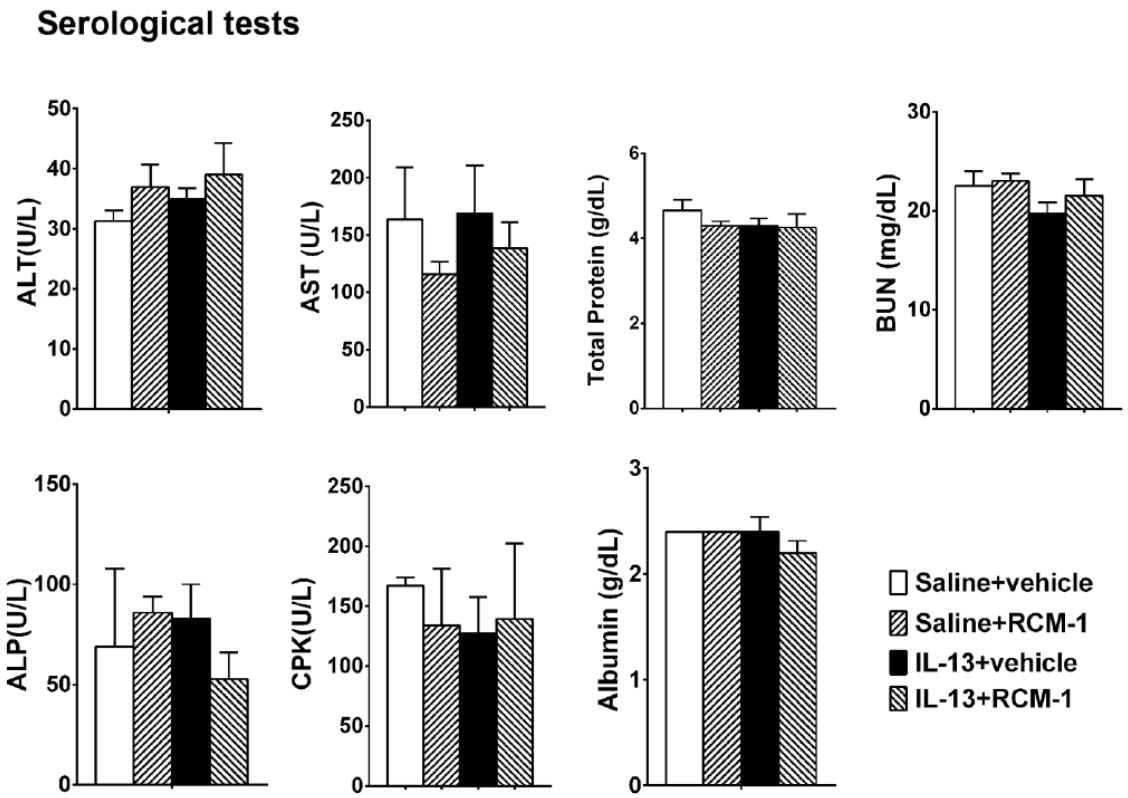

Fig. S7. Lack of toxicity of RCM-1 in IL-13–treated mice. IL-13 was given to BALB/c mice by intranasal administration on days 1, 3 and 4. RCM-1 was given by i.p. injection on days 0, 2 and 4. Serological analysis of blood serum was performed on day 5. RCM-1 did not affect ALT, AST, BUN, CPK, ALP, albumin and total protein in blood serum (n=4 mice per group). Data are shown as means ± standard errors of the means (SEM).

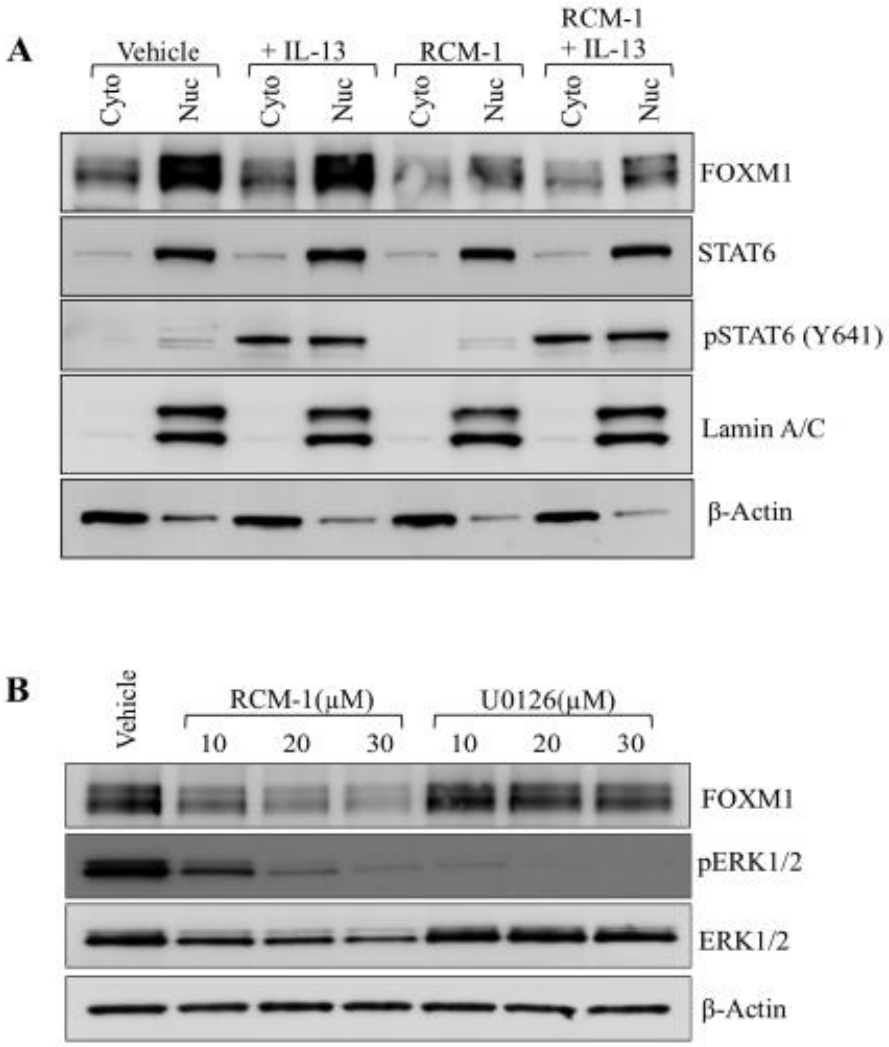

Fig. S8. RCM-1 inhibits nuclear accumulation of FOXM1 protein in A549 cells. (A) Western blot was performed using cytoplasmic and nuclear extracts from A549 cells. RCM-1 was added to cell cultures for 24hr. RCM-1 inhibits FOXM1 but does not change pSTAT6 and total STAT6 in nuclear and cytoplasmic extracts. Lamin A/C shows the purity of nuclear and cytoplasmic fractions (n=3 independent experiments). (B) Western blot showing dose-dependent responses of A549 cells to RCM-1 and U0126. Cells were treated with RCM-1 or U0126 for 24hr (n=3 independent experiments).

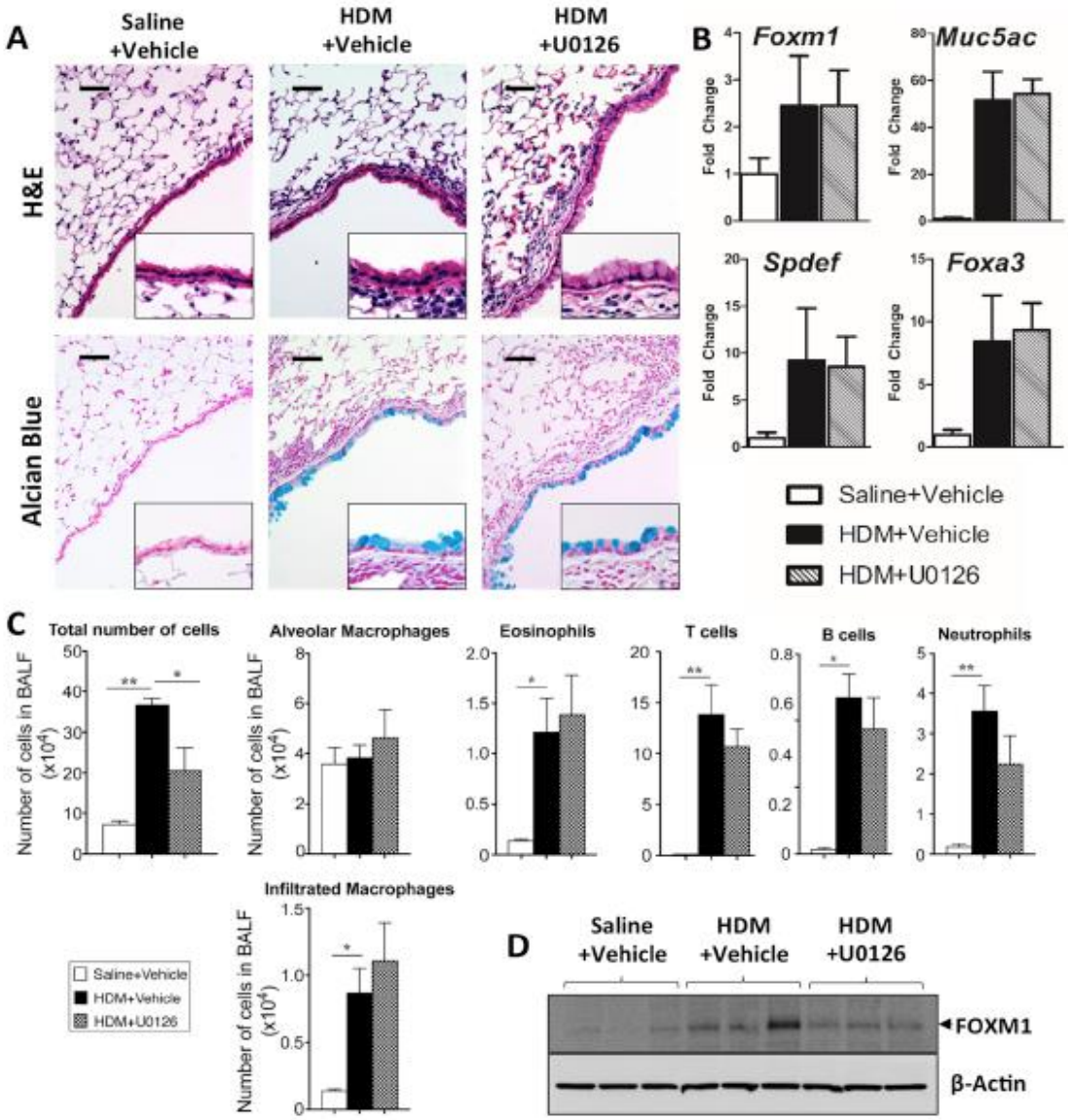

Fig. S9. U0126 decreases lung inflammation but does not affect goblet cell metaplasia or the abundance of FOXM1. (A) Lung paraffin sections were stained with H&E or Alcian blue. HDM was given to BALB/c mice by intranasal administration on days 0 and 14. U0126 was given by intraperitoneal injection on days 13, 15 and 16. Lungs were harvested 72h after the last HDM challenge. Scale bars are 50μm (images are representative of 3 mice per treatment). (B) qRT-PCR of total lung RNA shows that U0126 does not affect mRNA amounts of *Foxm1*, *Muc5ac*, *Spdef* and *Foxa3* in HDM-treated lungs (n=3 mice per group). (C) U0126 decreases the number of inflammatory cells in BALF. Total cell numbers were counted in BALF obtained from mice treated with HDM and U0126. BALF cell populations were identified by Flow cytometry after immunostaining for cell surface markers (n=3 mice in each group). (D) Total lung protein was analyzed by Western blot for endogenous FOXM1 and β-Actin. Each lane represents a different mouse.

Table S1. TaqMan assays for qRT-PCR.

Gene in TaqMan expression assay	Catalog no.
Human *FOXM1*	Hs00153543_m1
Mouse *Foxm1*	Mm01184444_g1
beta-Actin	Mm00607939_s1
Acta2	Mm00725412_s1
Agr2	Mm01291804_m1
Ccl2	Mm00441242_m1
Ccl11	Mm00441238_m1
Ccl20	Mm01268754_m1
Ccl24	Mm00444701_m1
Ccr2	Mm00438270_m1
Ccr3	Mm00515543_g1
Ccr6	Mm99999114_s1
Cx3cl1	Mm00436454_m1
Cx3cr1	Mm02620111_s1
Foxa2	Mm01976556_s1
Foxa3	Mm00484714_m1
Ifn-gamma	Mm01168134_m1
IL-4	Mm00445260_m1
IL-5	Mm00439646_m1
IL-12p35	Mm00434165_m1
IL-13	Mm00434204_m1
IL-25	Mm00499822_m1
IL-33	Mm00505403_m1
Ltc4s	Mm00521864_m1
Muc5ac	Mm01276718_m1
Ptgs2	Mm00478374_m1
Scgb1a1 (Ccsp)	Mm00442046_m1
Spdef	Mm00600221_m1

Table S2. Histological evaluation of inflammatory responses in lung tissue.

	Grade 0	Grade 1	Grade 2	Grade 3
Histological Variable				
Degree of inflammatory cell infiltration	Occasional mononuclear cells in the airway adventitia	Moderate cellular infiltration (lymphocytic, eosinophilic) of the bronchiolar adventitia with no or little infiltration of lamina propria	As in grade 1 but with increased cellular density and twofold thickness of the adventitia; mild epithelial infiltration; infiltrate lymphocytic, eosinophilic, or polymorphonuclear	Massive infiltration of either eosinophils or lymphocytes with increased polymorphonuclear cells at the periphery of the airway as well as adjacent blood vessels, between the smooth muscle fibers, within thelamina propria and epithelium
Vascular thickening/perivascular infiltrate	Normal intrapulmonary muscular arteries and pulmonary arteriole; no perivascular infiltrate	No changes to vascular wall but moderate perivascular infiltration of inflammatory cells	Hypertrophy of the media of muscular pulmonary arteries; moderate perivascular infiltration	As in grade 2 plus the proliferation of intimal cells and subendothelial fibrosis
Goblet cell metaplasia	Absent in terminal bronchioles; <10% of the epithelial cells within the bronchioles	<5% in the terminal bronchioles, <20% in the bronchioles and small bronchi	>10% goblet cells in the terminal bronchioles with >20% goblet cells in the bronchioles	>20% goblet cells in the terminal bronchioles and bronchioles
Alveolar septa thickening	Alveolar epithelium consisting of 1 thin layer	Increased cellular density of alveolar septum	Infiltration by inflammatory cells	Inflammatory cell infiltration and increased connective tissue deposition
Smooth muscle hypertrophy or hyperplasia	Bronchioles 1–2 discontinuous layers	Bronchioles 2–3 discontinuous layers	Bronchioles 3–4 discontinuous layers	Bronchioles >4 layers and dense
Peribronchiolar fibrosis	Loose connective tissue composing the adventitia	Increased fiber density without increase in adventitial thickness	Well-formed fibrous tissue accompanied by inflammatory cell infiltration; little involvement of lamina propria	Lamina propria and adventitia replaced by connective tissue and 2normal thickness

Table S3. Histology scores of lung tissue from HDM-treated mice. n=3 mice per treatment group.

Group	Mouse No.	Degree of inflammatory cell infiltration	Vascular thickening /perivascular infiltration	Goblet cell metaplasia	Alveolar septa thickening	Smooth muscle hypertrophy /hyperplasia	Peribronchiolar fibrosis	Combined scores
Saline +vehicle	1	1	0	0	0	0	0	1
	2	0	0	0	0	0	0	0
	3	0	0	0	0	0	0	0
Saline +RCM-1	4	0	0	0	0	0	0	0
	5	0	0	0	0	0	0	0
	6	0	0	0	0	0	0	0
HDM +vehicle	7	3	3	2	2	1	1	12
	8	3	3	1	1	1	0	9
	9	2	2	1	1	1	1	8
HDM +RCM-1	10	1	1	0	0	0	0	2
	11	1	1	0	0	0	0	2
	12	1	1	0	0	0	0	2